

See discussions, stats, and author profiles for this publication at: <https://www.researchgate.net/publication/261324210>

# Design, synthesis, molecular docking and 3D-QSAR studies of potent inhibitors of enoyl-acyl carrier protein reductase as potential antimycobacterial agents

ARTICLE · JANUARY 2014

---

CITATIONS

5

READS

10

## 6 AUTHORS, INCLUDING:



[Shrinivas D. Joshi](#)

S.E.T's College of Pharmacy, Dharwad, India

54 PUBLICATIONS 259 CITATIONS

[SEE PROFILE](#)



[Tejraj M Aminabhavi](#)

Texas State University

591 PUBLICATIONS 16,525 CITATIONS

[SEE PROFILE](#)



[Mallikarjuna N. Nadagouda](#)

United States Environmental Protection Ag...

162 PUBLICATIONS 3,788 CITATIONS

[SEE PROFILE](#)



[V.H. Kulkarni](#)

61 PUBLICATIONS 473 CITATIONS

[SEE PROFILE](#)



## Original article

# Design, synthesis, molecular docking and 3D-QSAR studies of potent inhibitors of enoyl-acyl carrier protein reductase as potential antimycobacterial agents



Uttam A. More <sup>a,b</sup>, Shrinivas D. Joshi <sup>a,\*</sup>, Tejraj M. Aminabhavi <sup>a</sup>, Andanappa K. Gadad <sup>c</sup>, Mallikarjuna N. Nadagouda <sup>a</sup>, Venkatrao H. Kulkarni <sup>a</sup>

<sup>a</sup> Novel Drug Design and Discovery Laboratory, Department of Pharmaceutical Chemistry, S.E.T's College of Pharmacy, Sangolli Rayanna Nagar, Dharwad 580 002, India

<sup>b</sup> Centre for Research and Development, Prist University, Thanjavur 613 403, Tamil Nadu, India

<sup>c</sup> School of Pharmacy, Faculty of Medical Sciences (The University of the West Indies, St. Augustine), Champs-Fleurs, Mount-Hope, Trinidad and Tobago

## ARTICLE INFO

## Article history:

Received 30 June 2013

Received in revised form

30 October 2013

Accepted 4 November 2013

Available online 11 November 2013

## Keywords:

CoMFA

CoMSIA

Pyrrole hydrazones

Anti-tubercular activity

Enoyl-ACP reductase subunit A

## ABSTRACT

In order to develop a lead antimycobacterium tuberculosis compound, a series of 52, novel pyrrole hydrazine derivatives have been synthesized and screened which target the essential enoyl-ACP reductase. The binding mode of the compounds at the active site of enoyl-ACP reductase was explored using surflex-docking method. The binding model suggests one or two hydrogen bonding interactions between pyrrole hydrazones and InhA enzyme. Highly active compound **5r** (MIC 0.2 µg/mL) showed hydrogen bonding interactions with Tyr158 and NAD<sup>+</sup> in the same manner as those of ligands PT70 and triclosan. The CoMFA and CoMSIA models generated with database alignment were the best in terms of overall statistics. The predictive ability of the CoMFA and CoMSIA models was determined using a test set of 13 compounds, which gave predictive correlation coefficients ( $r^2_{pred}$ ) of 0.896 and 0.930, respectively.

© 2013 Elsevier Masson SAS. All rights reserved.

## 1. Introduction

Tuberculosis (TB), is a major chronic infectious diseases caused by *Mycobacterium tuberculosis* (*M. tuberculosis*) and to a lesser degree by *Mycobacterium bovis* and *Mycobacterium Africanum*, affects nearly 32% of the World's population with about 9.4 million Worldwide and 1.6–2.4 million cases alone in India [1,2]. The disease has been the leading cause of morbidity and mortality among the infectious diseases. To address these issues, research and developmental activities to develop novel and potent new chemical entities are necessary.

InhA, the enoyl acyl carrier protein reductase (ENR) from *M. tuberculosis*, is one of the key enzymes involved in mycobacterial fatty acid elongation cycle, which has been validated as an effective antimicrobial target. Inhibition of mycolic acid biosynthesis is the first event detected in *M. tuberculosis* treated with isoniazid (INH)

[3], and numerous observations indicate that INH treatment causes extensive damage to the envelope organization, such as loss of acid-fast property [4], release of abnormal amount of proteins into the culture media and altered ultrastructure [5]. As a prodrug, INH must first be activated by KatG, a catalase-peroxidase that oxidizes INH to an acyl-radical which then forms a covalent adduct (INH-NAD) with NAD<sup>+</sup>, the co-substrate for InhA. The INH-NAD adduct then functions as a potent inhibitor of InhA [6].

Triclosan is present in a wide variety of consumer products, such as mouthwashes, toothpaste, and hand soaps [7], and is a widely used broad-spectrum biocide [8], despite its intravenous toxicity and biocidal component warranting against its systemic use [9]. Its active site entry results in the reordering of amino acids, making it a slow and tight-binding inhibitor [10] with a long residence time that is correlated with its *in vivo* activity [11].

Three-dimensional quantitative structure activity relationships (3D QSAR) methods, such as comparative molecular field analysis (CoMFA) [12] have been successfully applied to guide the design of new bioactive molecules [13]. The study has extended CoMFA and the more recently introduced comparative molecular similarity indices analysis (CoMSIA) [14,15] and other 3D QSAR

\* Corresponding author. Tel.: +91 9986151953; fax: +91 836 2467190.

E-mail addresses: [shrinivasdj@rediffmail.com](mailto:shrinivasdj@rediffmail.com), [shrinivasdj23@gmail.com](mailto:shrinivasdj23@gmail.com) (S. D. Joshi).

methodologies to potent antitubercular agents to gain better insights as to how steric, electrostatic, hydrophobic, and hydrogen-bonding interactions influence their activity, and thus derive the predictive 3D QSAR models for designing and forecasting the activity of InhA inhibitors of this class.

In the present study, design, synthesis, computation and evaluation of potential InhA inhibitors having pyrrole as the core structure are attempted. Other chemotherapeutically-active groups into the structure are introduced, with a hope to impart synergism to the target compounds (Fig. 1). Hydrazones, characterized by the presence of  $-\text{NH}-\text{N}=\text{C}-$  group, play an important role to exhibit antimicrobial activity [16]. Substituted carbohydrazone moiety has been found to be a good pharmacophore group for many antituberculosis active compounds [17–20]. However, some widely used antitubercular drugs such as thioacetazone, phtivazid, salinazid, verazide and opiniazide are also known to contain this group (Fig. 2).

As early as 1953, it was reported that some pyrrole derivatives showed *in vitro* antitubercular activity [21,22], but this keen observation was not given concerted follow-up at that time. More recently, major work has resumed on antitubercular drug design using pyrroles as templates for synthesis [23,24], including well-designed molecular modeling studies in conjunction with laboratory experiments [25–28]. Biava and co-workers have reported several 1,5-diarylpyrrole derivatives with very good activity against MTB (BM 212). On the basis of work by Deidda et al. [29], Lupin has synthesized a series of pyrrole compounds, one of which (LL3858) is currently in clinical development for the treatment of TB [30].

A database search shows that several pyrrole hydrazone derivatives have been developed against *M. tuberculosis* [23,24,31]. The main objective of this study is to design novel pyrrole hydrazone as specific inhibitors of *M. tuberculosis* and to further explore these entities as potential and novel antitubercular lead candidates. Earlier, we have reported antimycobacterial activity of pyrroles [24,27,28]. In continuation of these studies, the present

investigation deals with the development of potent antitubercular compounds with selective inhibition of enoyl acyl carrier protein reductase. Interest for this study stems from the presence of aryloxy moiety in many of the compounds, a common structural feature found in potent and potentially useful InhA inhibitors, such as 5-hexyl-2-(2-methylphenoxy)phenol (PT70 or TCU), 5-chloro-2-(2,4-dichloro phenoxy) phenol (TCL), a ligand in the published X-ray structure of InhA enzyme. In addition to 3D QSAR analyses, docking simulations were performed using the only published X-ray crystallographic structure of *M. tuberculosis* InhA (ENR) complexed with 5-hexyl-2-(2-methylphenoxy)phenol (PT70) and co-factor nicotinamide adenine dinucleotide ( $\text{NAD}^+$ ) (2X22 PDB) together with the available pharmacophore to explore the binding modes of these compounds at the InhA active site.

## 2. Molecular modeling/docking studies

The 3D structures were generated using SYBYL package (Tripos Associates, St. Louis, MO, USA) [32]. Using the standard bond lengths and bond angles, geometry optimization was carried out with the help of standard Tripos force field [33] with a distance dependent-dielectric function, energy gradient of 0.001 kcal/mol and MMFF94 as the electrostatics. Conformational analyses of all the 52 compounds were performed using a repeated molecular dynamics-based simulated annealing approach as implemented in Sybyl-X 2.0. The molecule was heated up to 1000 K within 2000 fs, held at this temperature for 2000 fs and annealed to 0 K for 10,000 fs using an exponential annealing function. By applying this procedure, a total of 100 conformations were sampled out during the 100 cycles to account for conformational flexibility to find the most likely conformations occurring most often in the resulting pool. All the conformations were then minimized with Tripos force field and atomic charges were calculated using the MMFF94 (Merck Molecular Force Field) method.

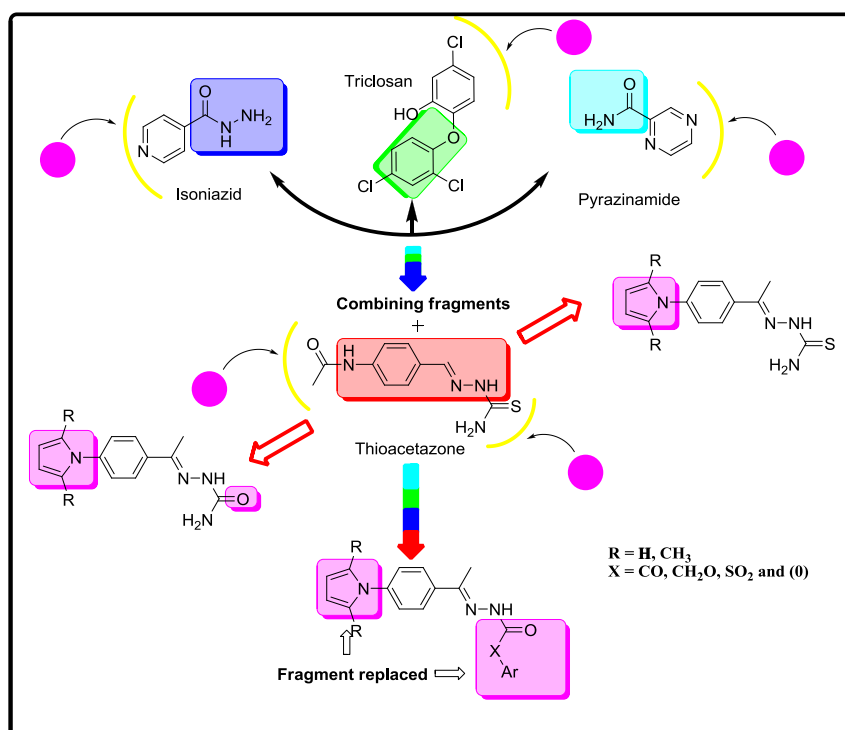
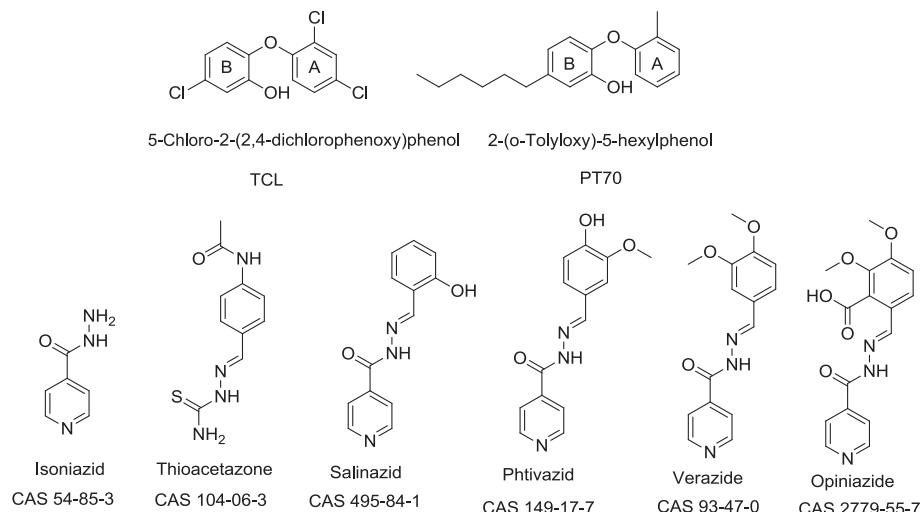


Fig. 1. Design concept for pyrrole hydrazone derivatives.



**Fig. 2.** Chemical structures of tricosan (TCL) and its analog PT70; some hydrazide and hydrazones used as tuberculostatics.

### 2.1. Data set and structures

The *in vitro* antitubercular activity (expressed as MIC) was converted into pMIC (log MIC) values, which were used to construct the 3D-QSAR models. Structures and biological activities of the compounds are summarized in Table 1. The 3D-QSAR models were generated using a training set of 39 molecules, and the predictive power of the resulting models was evaluated using a test set of 13 molecules. Test compounds were selected randomly such that the data set included diverse structures and a wide range of activity.

### 2.2. Alignment rule

A common substructure-based alignment was adopted, wherein the molecules were aligned to the template molecule on a common backbone as illustrated in Fig. 3A and B. For database alignment of the inhibitors, the structure of compound **5r** was used as a template.

### 2.3. CoMFA and CoMSIA settings

The CoMFA [17] descriptors, steric (Lennard-Jones 6–12 potential) and electrostatic (Coulombic potential) field energies were calculated using the standard parameters i.e.,  $sp^3$  carbon probe atom with +1 charge, van der Waals radius of 1.52 Å and energy cutoff of 30 kcal/mol. The CoMSIA [14,15] similarity indice descriptors (steric, electrostatic, hydrophobic, H-bond donor and H-bond acceptor fields) were calculated using a probe with a radius of 1.0 Å and a default value of 0.3 as the attenuation factor. A grid spacing of 2 Å was used for both CoMFA and CoMSIA. The  $q^2$  resulted in an optimum number of components and the lowest standard error of prediction. The equations for  $q^2$  and standard errors are given below.

$$q^2 = 1 - \frac{\sum_y (\mathbf{Y}_{\text{pred}} - \mathbf{Y}_{\text{actual}})^2}{\sum_y (\mathbf{Y}_{\text{actual}} - \mathbf{Y}_{\text{mean}})^2} \quad (1)$$

where  $\mathbf{Y}_{\text{pred}}$  is the predicted activity,  $\mathbf{Y}_{\text{actual}}$  is the experimental activity and  $\mathbf{Y}_{\text{mean}}$  is the best estimate of the mean.

$$\text{SEE, SEP} = \sqrt{\frac{\text{PRESS}}{n - c - 1}} \quad (2)$$

Here,  $n$  is the number of compounds,  $c$  is the number of components and

$$\text{PRESS is calculated as } = \sum_y (\mathbf{Y}_{\text{pred}} - \mathbf{Y}_{\text{actual}})^2 \quad (3)$$

Similarity index  $A_{F,k}$  for a molecule,  $j$  with atoms at the grid point  $q$  was calculated as:

$$A_{F,k}^q(j) = \sum_i \omega_{\text{probe},k} \omega_{ik} e^{-\alpha r_{iq}^2} \quad (4)$$

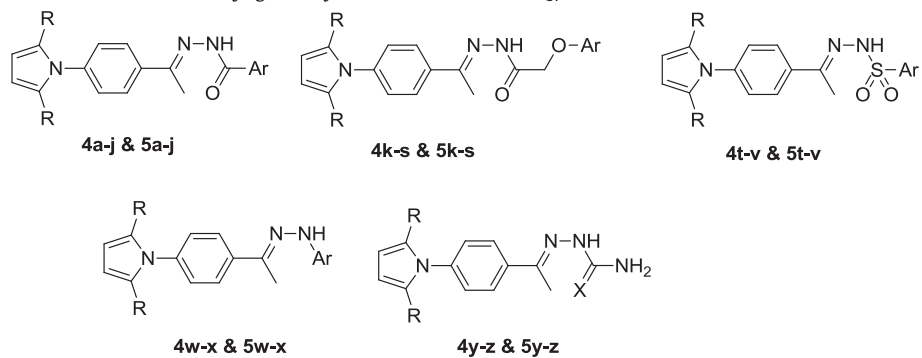
where  $\omega_{\text{probe},k}$  is the probe atom with radius 1 Å, charge +1, hydrophobicity +1, hydrogen bond donating +1 and hydrogen bond accepting +1;  $\omega_{ik}$  is actual value of the physicochemical property  $k$  of atom  $i$ ;  $r_{iq}$  is the mutual distance between the probe atom at grid point  $q$  and atom  $i$  of the test molecule;  $\alpha$  is attenuation factor, while the default value of  $\alpha$  is 0.3. Five physicochemical properties  $k$  (steric, electrostatic, hydrophobic, hydrogen bond acceptor and donor) were evaluated using a common charged, hydrophobic and hydrogen bond accepting probe atom.

### 2.4. Partial least squares (PLS)

The CoMFA and CoMSIA descriptors were used as independent variables and pMIC as the dependent variable in the partial least squares (PLS) analysis to derive the 3D-QSAR models. The optimal number of components was determined with SAMPLS [34] (samples-distance partial least squares) and cross-validation was carried out by the leave-one-out method. The model with optimum number of components (highest  $q^2$ ) and with the lowest standard error of prediction was considered for further analysis. To further assess robustness and statistical confidence of the derived models, bootstrapping [35] analysis for 100 runs was performed. To test the predictive power of the derived CoMFA and CoMSIA models, biological activities of the test set molecules were predicted using the models derived from the training set. The pMIC values that are unbiased by the mean of the test set representing the external predictivity were calculated.

### 2.5. Predictive ability of CoMFA and CoMSIA models ( $r_{\text{pred}}^2$ )

Predictive ability of each analysis was determined from the test set molecules that were not included in the training set. These

**Table 1**Data set of chemical structures and antitubercular activity against *Mycobacterium tuberculosis* H<sub>37</sub>RV:

Compd	R	Ar	X	MIC µg/mL	Compd	R	Ar	X	MIC µg/mL
<b>4a</b>	H		—	50	<b>5a</b>	CH <sub>3</sub>		—	100
<b>4b</b>	H		—	50	<b>5b</b>	CH <sub>3</sub>		—	100
<b>4c</b>	H		—	12.5	<b>5c</b>	CH <sub>3</sub>		—	50
<b>4d</b>	H		—	25	<b>5d</b>	CH <sub>3</sub>		—	25
<b>4e</b>	H		—	50	<b>5e</b>	CH <sub>3</sub>		—	25
<b>4f</b>	H		—	50	<b>5f</b>	CH <sub>3</sub>		—	25
<b>4g</b>	H		—	50	<b>5g</b>	CH <sub>3</sub>		—	25
<b>4h</b>	H		—	50	<b>5h</b>	CH <sub>3</sub>		—	25
<b>4i</b>	H		—	25	<b>5i</b>	CH <sub>3</sub>		—	12.50
<b>4j</b>	H		—	12.5	<b>5j</b>	CH <sub>3</sub>		—	25
<b>4k</b>	H		—	12.5	<b>5k</b>	CH <sub>3</sub>		—	0.8
<b>4l</b>	H		—	12.5	<b>5l</b>	CH <sub>3</sub>		—	3.125
<b>4m</b>	H		—	12.5	<b>5m</b>	CH <sub>3</sub>		—	3.125
<b>4n</b>	H		—	50	<b>5n</b>	CH <sub>3</sub>		—	6.25
<b>4o</b>	H		—	25	<b>5o</b>	CH <sub>3</sub>		—	50
<b>4p</b>	H		—	25	<b>5p</b>	CH <sub>3</sub>		—	25

**Table 1** (continued)

Compd	R	Ar	X	MIC µg/mL	Compd	R	Ar	X	MIC µg/mL
<b>4q</b>	H		—	50	<b>5q</b>	CH <sub>3</sub>		—	12.5
<b>4r</b>	H		—	0.4	<b>5r</b>	CH <sub>3</sub>		—	0.2
<b>4s</b>	H		—	0.2	<b>5s</b>	CH <sub>3</sub>		—	0.2
<b>4t</b>	H		—	0.8	<b>5t</b>	CH <sub>3</sub>		—	0.4
<b>4u</b>	H		—	0.2	<b>5u</b>	CH <sub>3</sub>		—	0.8
<b>4v</b>	H		—	6.25	<b>5v</b>	CH <sub>3</sub>		—	12.5
<b>4w</b>	H		—	12.50	<b>5w</b>	CH <sub>3</sub>		—	25
<b>4x</b>	H		—	12.50	<b>5x</b>	CH <sub>3</sub>		—	12.5
<b>4y</b>	H	—	S	50	<b>5y</b>	CH <sub>3</sub>	—	S	50
<b>4z</b>	H	—	O	100	<b>5z</b>	CH <sub>3</sub>	—	O	50
Isoniazid				0.25		Triclosan			10

molecules were aligned and their activities were predicted by each PLS analysis. The predictive  $r^2$  ( $r^2_{\text{pred}}$ ) value is defined as:

$$r^2_{\text{pred}} = \frac{(\text{SD} - \text{PRESS})}{\text{SD}} \quad (5)$$

where SD is the sum of squared deviations between the biological activities of the test set and the mean activity of the training set molecules, while PRESS is the sum of squared deviation between the actual and predicted activities of the test set molecules, calculated by Eq. (3)

## 2.6. Molecular docking using Surflex-Dock

The 3D-QSAR is only a kind of ligand-based approach, but the robustness of the derived models is greatly affected by the diversity of the molecules in the data set. Thus, information received from the 3D-QSAR analysis is relatively limited. Therefore, molecular docking was used to further clarify the binding mode of the compounds to provide straightforward information for further structural optimization. Surflex-Dock that adopted an empirical scoring function and a patented search engine [36,37] was employed for molecular docking study. The crystal structure of *M. tuberculosis* InhA inhibited by PT70

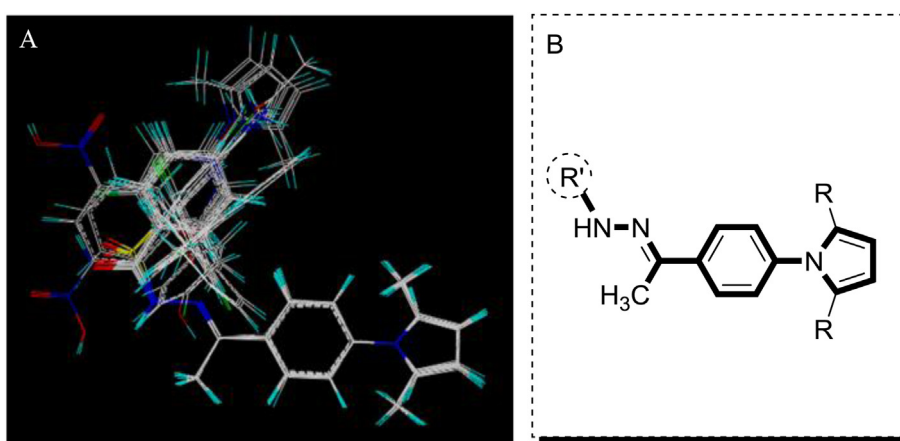


**Fig. 3.** A) Database alignment of the 52 studied molecules. B) Common core structure for alignment is shown in bold.

(PDB entry code 2X22) was extracted from the Brookhaven Protein Database (PDB <http://www.rcsb.org/pdb>). During the docking process, water molecules and all the ligands in the crystal structures were removed (except co-factor NAD<sup>+</sup>), and the polar hydrogens as well as united atom Amber7FF99 were assigned for the protein {PDB code 2X22 (chain A)}. Then, ligand-based mode was adopted to generate the “protomol”, leaving the threshold and bloat parameters at their default values of 0.50 and 0 Å, respectively. Then, all the inhibitors were docked within the prepared protein.

The mode of interaction of the relative ligand (PT70 and triclosan) in the crystal structure against 2X22 PDB was used as a standard docked model. The maximum number of poses per ligand was set to 20 and no constraints were used to perform molecular docking. The docking complex assumed to represent ligand–receptor interactions was selected based on three criteria: (i) docking score of the pose possessed the highest docking score, (ii) its orientation of aromatic rings of the ligand oriented into the active site in a similar manner with the cocrystallized ligands orientation, and (iii) the preservation of two key interactions, namely hydrogen bonds with Tyr158 and co-factor NAD<sup>+</sup>. For a comparative analysis of the designed molecules, G\_score [38], PMF\_score [39], D\_score [40] and Chem\_score [41] were estimated using C-Score module of the Sybyl-X 2.0.

### 3. Results and discussion

#### 3.1. Chemistry

Studies were undertaken to synthesize the novel pyrrole ring bearing hydrazone derivatives to investigate their antitubercular effects. Compounds **4a–z** and **5a–z** were synthesized as per Scheme 1. Pyrrole synthesis is achieved via a *paal-knorr* mechanism by the condensation of 2,5-dimethoxytetrahydrofuran or 1,4-diketone (2,5-hexanedione) and *p*-aminoacetophenone in the presence of dry acetic acid to get 4-(1*H*-pyrrol-1-yl)-acetophenone (**2**) or 4-(2,5-dimethyl-1*H*-pyrrol-1-yl)-acetophenone (**3**) in good yield. Commercially available acids **7a–j** and synthesized aryloxy acetic acids **7k–s** were successfully converted to acid hydrazides **9a–s** by a sequential esterification and hydrazinolysis. Some sulfonyl hydrazides **11t–v** were prepared by the reaction of sulfonyl chloride **10t–u** with hydrazine hydrate in dichloromethane (Scheme 2). The commercially available phenyl hydrazine hydrochloride, 2,4-dinitrophenyl hydrazide, thiosemicarbazide and semicarbazide hydrochloride were purified with suitable solvents and used in the synthesis. The NH<sub>2</sub> in hydrazides is more nucleophilic than NH, which reacts preferentially with the more reactive carbonyl group, leading to the formation of hydrazone derivatives **4a–z** or **5a–z** as major products specially if the reaction is carried out in the presence of a catalytic amount of acetic acid or TFAA upon heating and without heating.

The structures of **2** and **3** were established by FTIR and NMR. The compounds **2** and **3** showed characteristic absorption bands at 1666 cm<sup>−1</sup> and 1667 cm<sup>−1</sup> for carbonyl group and the absence of NH stretching band around 3400–3250 cm<sup>−1</sup>. The <sup>1</sup>H NMR spectrum for **2** showed a singlet at δ 2.59 ppm, representing three protons of CH<sub>3</sub> group and two triplets at δ 6.33 (C<sub>3</sub>, C<sub>4</sub>—H) and 7.30 (C<sub>2</sub>, C<sub>5</sub>—H) ppm for four pyrrole methine protons of coupling constant, *J* = 2.24 Hz, confirming the presence of pyrrole moiety. Two multiplets at δ 7.56–7.60 and 7.97–8.04 ppm for C<sub>3</sub>, C<sub>5</sub>—H and C<sub>2</sub>, C<sub>6</sub>—H four protons of phenyl ring are observed. The characteristic carbonyl peak observed at δ 196.21 ppm in <sup>13</sup>C NMR spectrum of **2** and <sup>1</sup>H NMR spectrum of **3** showed singlets at δ 1.99 and 2.63 ppm, representing the six methyl protons of 2,5-dimethyl pyrrole and three protons of ketonic methyl group, respectively. A singlet at δ 5.84 ppm is also observed due to two protons of pyrrole C<sub>3</sub> and C<sub>4</sub>—H. Aromatic protons of phenyl ring C<sub>3</sub>, C<sub>5</sub> and C<sub>2</sub>, C<sub>6</sub>—H

appeared as two doublets at 7.43 and 8.10 ppm with coupling constants of *J* = 8.40 and 8.70, respectively. The peak at δ 197.60 ppm in the <sup>13</sup>C NMR spectrum of **3** is characteristic of the carbonyl group.

Hydrazone derivatives were confirmed by FTIR spectral data that showed characteristic peaks in the range 3369–3169 cm<sup>−1</sup>, indicating the presence of NH group, and a sharp peak around 1513–1620 cm<sup>−1</sup> indicates the presence of C=N group. The <sup>1</sup>H NMR showed singlets in the range of δ 9.15–11.29 ppm corresponding to —NH—N= proton in the products, which vanished upon D<sub>2</sub>O exchange. A singlet at 1.99–2.03 ppm and δ 2.20–2.53 ppm in the <sup>1</sup>H NMR spectra of the compounds indicate the presence of two methyl groups at 2nd and 5th positions of pyrrole and ketonic (—N=C—CH<sub>3</sub>) protons, respectively. The peaks at δ 196.21 or 197.60 ppm (C=O of pyrrolyl acetophenone) are absent in <sup>13</sup>C NMR spectra of the products. The mass spectra also confirm the structures of the products.

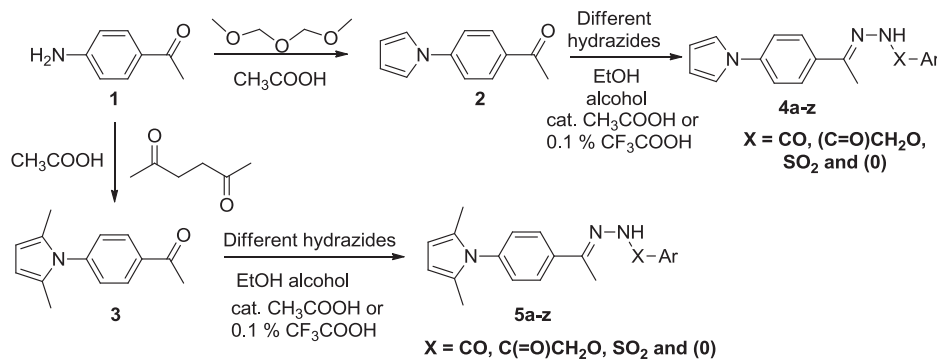
#### 3.2. MIC and cytotoxicity

The MIC values of the compounds against the selected *M. tuberculosis* H<sub>37</sub>Rv are given in Table 1. The tested compounds (**4a–z** and **5a–z**) showed activities against mycobacteria with the MIC values ranging from 0.2 to 100 µg/mL. Compounds **4r–u**, **5k** and **r–u** inhibited mycobacterial growth very effectively compared to others in the series with MIC values ranging from 0.2 to 0.8 µg/mL. Certain therapeutic properties are required to be identified if an antimycobacterial compound has the potential as a drug. Toxicity is one of these important criteria. Hence, we have investigated the potential toxicity of the six selected pyrrole hydrazones (**4r**, **s**, **u** and **5r–t**) towards mammalian Vero cell-lines and A<sub>549</sub> (lung adenocarcinoma) cell-lines up to concentrations of 62.5 µg/mL. Among the tested compounds, **5t** showed inferior toxicity with IC<sub>50</sub> values of 279 µM against mammalian Vero cell-lines, while other compounds (**4r**, **s**, **u**, **5r** and **s**) showed IC<sub>50</sub> values ranging from 240 to 277 µM against both mammalian Vero cell-lines and A<sub>549</sub> (lung adenocarcinoma) cell-lines (see Table 2).

#### 3.3. Molecular modeling

Docking studies with Surflex-Dock showed that the synthesized compound **5r** occupy the same binding site as that of PT70 and TCL (Fig. 4). The PT70 showed two hydrogen bonding interactions, the oxygen of hydroxy group on ring B makes hydrogen bonds with that of OH of the active site of NAD<sup>+</sup> ribose (1.8 Å), while hydrogen of hydroxy group on ring B makes hydrogen bonds with OH of the active site Tyr<sub>158</sub> (1.8 Å). In case of **5r**, which is composed of a 1-naphthoxy ring and a 2,5-dimethyl-1*H*-pyrrol-1-yl phenyl ring linked by a hydrazone moiety, the 1-naphthoxy core moiety occupies the same space in the substrate binding site as does the ring A of PT70 and triclosan and thus, makes a stacking interaction with the ribose ring of NAD<sup>+</sup> (Fig. 5A and B). Such a stacking interaction is very important and has been conserved in all the ENRs for which crystal structures have been solved with NAD<sup>+</sup> and PT70 in ternary complex with the enzyme. The NH group makes hydrogen bonding interaction with the oxygen of aromatic hydroxy group of Tyr<sub>158</sub> (2.1 Å). The oxygen of carbonyl group makes hydrogen bonds with the hydrogen of OH group of the active site of ribose NAD<sup>+</sup> (2.3 Å).

Compound **4r** is composed of three rings: a pyrrole ring at one end, a 1-naphthoxy moiety at the other end, and one phenyl ring in the middle with the hydrazone bridge. The modeling suggests that compound **4r** binds to the subunit A of InhA (NAD<sup>+</sup> (2.2 Å) and Tyr<sub>158</sub> (2.2 Å)) with a binding model similar to that of **5r**. However, TCL showed the same hydrogen bonding interactions (NAD<sup>+</sup> (2.0 Å) and Tyr<sub>158</sub> (1.8 Å)) as that of PT70. All ligands with docked



$X = \text{C(=O)}$	$X = \text{C(=O)CH}_2\text{O}$	$X = \text{SO}_2$	$X = (\text{O})$
$4\text{a}, 5\text{a}$	$4\text{k}, 5\text{k}$	$4\text{t}, 5\text{t}$	$4\text{w}, 5\text{w}$
$4\text{b}, 5\text{b}$	$4\text{l}, 5\text{l}$	$4\text{u}, 5\text{u}$	$4\text{x}, 5\text{x}$
$4\text{c}, 5\text{c}$	$4\text{m}, 5\text{m}$	$4\text{v}, 5\text{v}$	
$4\text{d}, 5\text{d}$	$4\text{n}, 5\text{n}$		
$4\text{e}, 5\text{e}$	$4\text{o}, 5\text{o}$		$4\text{y}, 5\text{y} \ X = \text{C(=S)NH}_2$
$4\text{f}, 5\text{f}$	$4\text{p}, 5\text{p}$		$4\text{z}, 5\text{z} \ X = \text{C(=O)NH}_2$
$4\text{g}, 5\text{g}$	$4\text{q}, 5\text{q}$		
$4\text{h}, 5\text{h}$	$4\text{r}, 5\text{r}$		
$4\text{i}, 5\text{i}$			
$4\text{j}, 5\text{j}$	$4\text{s}, 5\text{s}$		

**Scheme 1.** Synthetic route of a novel series of pyrrole hydrazone derivatives.

alignment and fast Connolly surface of the active site of InhA enzyme have shown in Fig. 6A and B).

The C-score (Consensus score) indicating the summary of all the forces of interaction between the ligands and InhA enzyme, including the crash score is in favor of all the synthesized compounds in the series, followed by triclosan and PT70 (Table 3). Charge and van der Waals interactions between the protein and the ligand suggests that **5r**, **4r**, **5q**, **s** and **d** are the superior ligands than PT70, triclosan and other compounds to bind with ENRs. Helmholtz free energies of interactions for protein–ligand atom pairs have more preference to all the compounds over those of PT70 and triclosan.

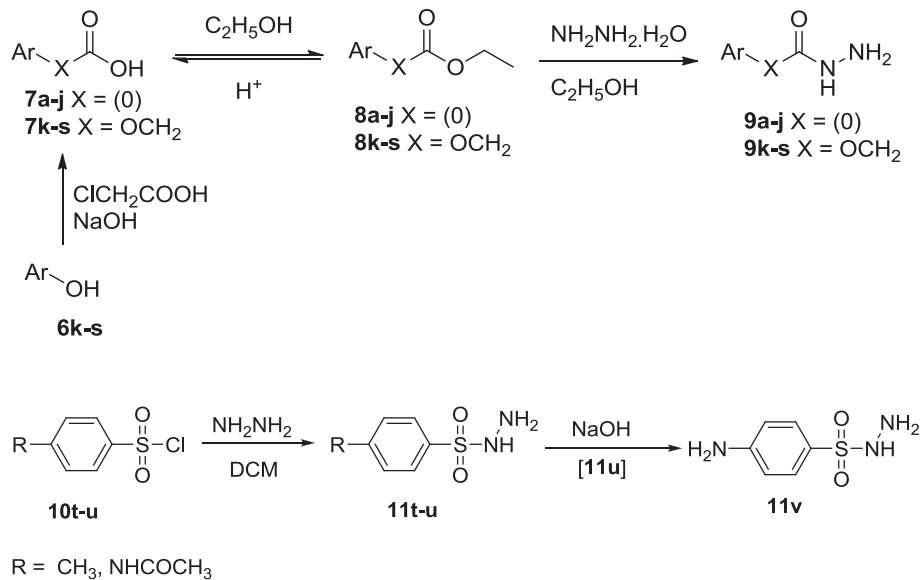
Compounds **5r**, **q** and **s** showed better hydrogen bonding, complex (ligand–protein), and internal (ligand–ligand) energies than PT70, triclosan and other compounds in the series. Scoring of compounds

with respect to the reward for hydrogen bonding, lipophilic contact, and rotational entropy, along with intercept terms reveals that compounds **5r**, **4r** and **5s** showed increased interactions with the protein than PT70, triclosan and other compounds.

In conclusion, *in vitro* studies demonstrated that **5r**, **4s**, **5s** and **4u** exhibit promising anti-tubercular activity with less toxicity. Molecular modeling and docking studies suggest that compounds **5r**, **4r** and **5l** interact with InhA enzyme more efficiently and hence, these can be further developed to improve their antitubercular activity.

### 3.4. CoMFA and CoMSIA models

The data set of the newly synthesized pyrrole hydrazone antitubercular agents was used to perform 3D-QSAR studies. During optimization of 3D-QSAR models, variations of parameters such



Scheme 2. Synthetic route for the preparation of different hydrazides.

as grid spacing and attenuation factor were considered and the best results were obtained from the parameters with the default values the CoMFA and CoMSIA studies with the molecules were aligned by docking at the active site in the horizontal binding region. The docked alignment was quite different as the molecules were more staggered and so, only few compounds were docked differently from the rest of the compounds. The CoMFA and CoMSIA 3D QSAR models with a positive, albeit low  $q^2$  values of 0.179 and 0.305 with 3 and 5 PLS components, respectively.

Table 4 shows the results with 52 compounds in the docked alignment. All the molecules split into two sets, training and test set by chemical diversity method to perform the 3D QSAR study on both the docked alignment and the database alignment. The final better QSAR model was obtained with database alignment. CoMFA PLS analyses of 39 molecules of training set resulted in  $q^2$  values of 0.341 and 0.667 and  $r^2$  values of 0.769 and 0.922 for the docked alignment and database alignment conformational sets, respectively (Table 4).

CoMSIA PLS analysis of the training set using the antitubercular activity as a response variable afforded models with  $q^2$  values of 0.373 (docked alignment) and 0.599 (database alignment), and  $r^2$  values of 0.693 and 0.920 for the docked alignment and database alignment sets, respectively (Table 4). The CoMSIA was a better QSAR model than CoMFA with docked alignment as indicated by the  $q^2$  values and the number of compounds that could be

accommodated, indicating that CoMSIA model was less affected by the alignment heterogeneity.

The plots of predicted vs actual pMIC values for the database aligned training and test sets are shown in Fig. 7 for both CoMFA and CoMSIA models. The actual, predicted pMIC values and residuals from the prediction of the training and test set compounds by the database alignment for CoMFA and CoMSIA models are shown in Table 5.

### 3.5. Contour maps

**Steric field.** Green contour plots indicate regions where the bulky groups are associated with increased bioactivity, while the yellow contour plots indicate regions where such bulky groups are not favoring bioactivity. Figs. 8A and 9A show that 1-naphthoxy group of compound 5r (pMIC = 6.699, C-Score = 10.98) is oriented toward the green polyhedron where the bulky groups are favored as per the obtained model. Meanwhile, the other CH<sub>3</sub> group of pyrrole and ketonic methane is located relatively far away from the yellow color contour. In addition, relatively small yellow color contours in the region of nicotinoyl or benzoyl indicated that significantly small bulky substituents decrease the bioactivity, as for example, in the case of 5a (pMIC = 4.000, C-Score = 7.69) derivative.

**Electrostatic field.** The red contours indicate regions in which the presence of negative charge increases the activity, while the blue contours show regions where the negative charge is not favored.

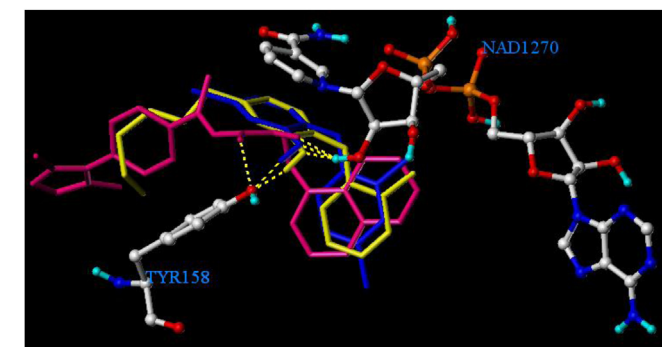


Fig. 4. Overlay of 5r (pink), PT70 (yellow) and TCL (Blue) with the crystal structure of a cofactor NAD<sup>+</sup> and Tyr158 in InhA. (For interpretation of the references to color in this figure legend, the reader is referred to the web version of this article.)

Table 2  
Cytotoxicity activity of selected pyrrole hydrazone derivatives.

Compound	IC <sub>50</sub> ( $\mu\text{M}$ ) <sup>a</sup>	
	MV cell-lines <sup>b</sup>	A <sub>549</sub> <sup>c</sup>
4r	240 ± 0.2	243 ± 0.2
4s	249 ± 0.2	247 ± 0.3
4u	263 ± 0.2	257 ± 0.2
5r	277 ± 0.3	269 ± 0.2
5s	255 ± 0.4	260 ± 0.3
5t	279 ± 0.3	277 ± 0.3
Isoniazid	>450	>450
Cisplatin	1.29	9.90

<sup>a</sup> Cytotoxicity is expressed as IC<sub>50</sub> which is the concentration of compound reduced by 50% of the optical density of treated cells with respect to untreated cells using MTT assay. Values are the means ± SEM of three independent experiments.

<sup>b</sup> Mammalian Vero cell-lines.

<sup>c</sup> A<sub>549</sub> (lung adenocarcinoma) cell-lines.

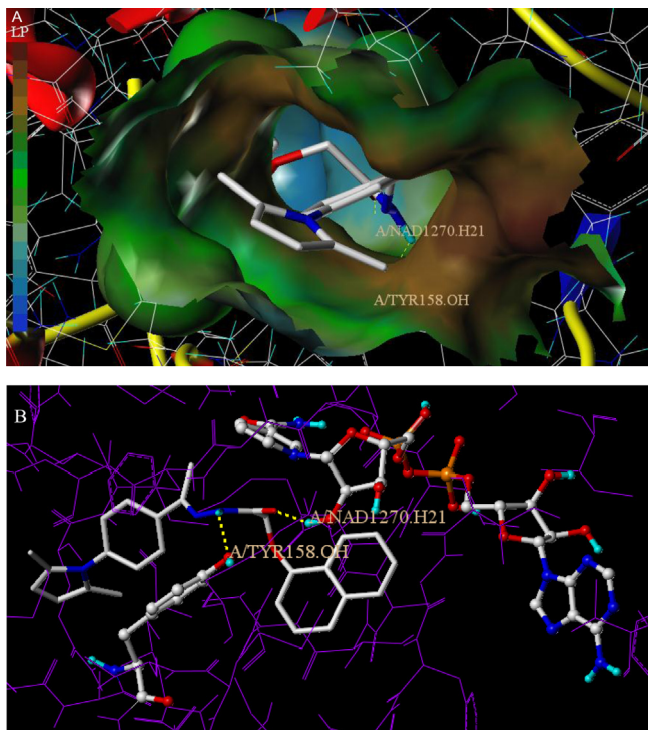


**Fig. 5.** (A) Docking conformation of the most potent inhibitor **5r** and corresponding fast Connolly surface at the ENR site with lipophilic property (B) the interactions between ENR site and compound **5r**.

The contribution of oxygen (chlorine, bromine) to the activity due to electrostatic field in compound **5r** is eminent as shown in Figs. 8B and 9B. Such a contribution is lacking for **4w** ( $p\text{MIC} = 4.903$ , C-Score = 7.38), **5w** ( $p\text{MIC} = 4.602$ , C-Score = 9.42), **4y** ( $p\text{MIC} = 4.301$ , C-Score = 4.91) and **5y** ( $p\text{MIC} = 4.301$ , C-Score = 6.01). However, the blue polyhedron in the region of NH of hydrazone and surrounding aromatic protons is due to the favoring effect of hydrazone group (N atom).

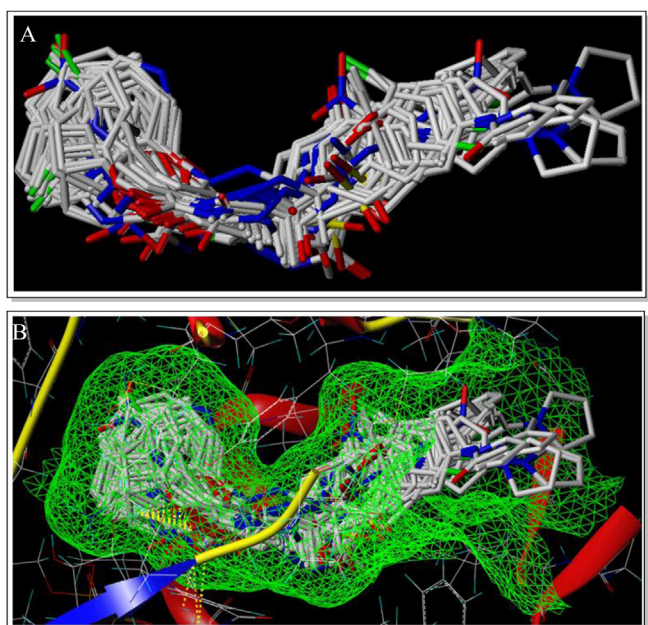


**Fig. 6.** (A) All ligands with docked alignment B) binding pocket of InhA enzyme with alignment of docked conformations.

**Hydrophobicity field.** According to CoMSIA model, as shown in Fig. 9C, hydrophobicity is favored in aroyloxy or aryl (yellow contour), while O atom of phenoxy and methylene group ( $\text{OCH}_2$ ) coincides with the gray contour emphasizing the favoring effect of a hydrophilic substituent.

**Hydrogen-bond-acceptor field.** In Fig. 9D, it can be observed that in the highly active template molecule **5r**, the magenta contour in the region of hydrazone bridge coincides with the oxygen atom of  $-\text{C=O}$  and  $-\text{C}-\text{O}-\text{C}-$  groups favored for activity.

**Hydrogen-bond-donor field.** In Fig. 9E, cyan contour on the NH and also on the aromatic ring protons of molecule **5r** favor activity.

### 3.6. Predictions for the test set

The obtained database aligned CoMFA and CoMSIA models, which comprised of steric, electrostatic, hydrophobic, H-bond acceptor and H-bond donor fields to predict the activity of 13 compounds of the test set. The activity results of CoMFA and CoMSIA model predictions of these compounds were quite satisfactory. The bioactivity of compounds **4x**, **z**, **5b**, **i**, **n**, **u**, **w** and **y** were also predicted satisfactorily both by CoMFA and CoMSIA models with the residuals of  $0.054/-0.043$ ,  $-0.627/-0.482$ ,  $-0.597/-0.49$ ,  $0.047/0.139$ ,  $-0.046/0.081$ ,  $-0.511/-0.731$ ,  $-0.367/0.143$ ,  $-0.258/0.053$ , respectively. In addition, the bioactivity of compound **4t** was predicted satisfactorily by CoMSIA model ( $0.441/-0.012$ ). On the other hand, both the models did not predict satisfactorily the activity of compounds **4a**, **j**, **m** and **w**, which possess 2,5-unsubstituted pyrrole ring with the residuals of  $0.233/0.262$ ,  $0.168/0.631$ ,  $0.297/0.163$ ,  $0.243/0.686$ , respectively.

## 4. Experimental section

Melting points were determined using the Shital-digital programmable melting point apparatus and are uncorrected. FTIR spectra in KBr pellets were recorded on a Bruker FTIR spectrophotometer. The  $^1\text{H}$  and  $^{13}\text{C}$  NMR spectra were recorded on a Bruker AVANCE II at 400 and 100/75 MHz, respectively; chemical shifts are expressed in parts per million (ppm) relative to TMS. The abbreviations used to describe the peak patterns are: (b) broad, (s) singlet, (d) doublet, (t) triplet, (q) quartet, and (m) multiplet. Mass spectra (MS) were recorded in a JEOL GCMATE II GC-Mass spectrometer and Schimadzu QP 2010S GC-Mass spectrometer. Elemental analysis data (performed on Leco Tru Spec CHNS Analyzer) for C, H, and N were within  $\pm 0.4\%$  of the theoretical values. Analytical thin-layer chromatography (TLC) was performed on precoated TLC sheets of silica gel 60 F<sub>254</sub> (Merck, Darmstadt, Germany) visualized by long- and short-wavelength ultraviolet (UV) lamps. Chromatographic purifications were performed on Merck aluminum oxide (70–230 mesh) and Merck silica gel (70–230 mesh).

### 4.1. General procedure for the synthesis of aryloxy acetic acids (**7k–s**)

Equimolar quantities of chloroacetic acid (0.05 mol) and appropriate phenol (**6k–s**) (0.05 mol) were taken in a conical flask, to which aqueous solution of NaOH (0.12 mol in 25 mL water) was slowly added with constant stirring. The solution was stirred for 2 h until the solution turned clear, brown or yellow and then the reaction mixture was evaporated in an evaporating dish until the solid sodium salt was precipitated. The salt was isolated, dried, dissolved in water and acidified by adding con. HCl. The precipitated aryloxy acetic acid was filtered and recrystallized from water or ethanol.

**Table 3**

Surflex-Dock scores (kcal/mol) of pyrrole hydrazone derivatives.

Compd	C score <sup>a</sup>	Crash score <sup>b</sup>	Polar score <sup>c</sup>	D score <sup>d</sup>	PMF score <sup>e</sup>	G score <sup>f</sup>	Chem score <sup>g</sup>
PT70	13.60	-0.96	2.13	-168.341	-42.822	-307.070	-48.411
5r	10.98	-3.07	0.80	-207.176	-61.325	-376.075	-54.517
4r	10.56	-2.38	0.82	-199.019	-65.418	-345.764	-50.632
5l	10.12	-2.03	0.03	-182.103	-59.135	-309.089	-45.513
4l	9.78	-1.87	0.36	-172.803	-50.176	-300.107	-43.459
5q	9.60	-3.33	0.00	-210.443	-66.278	-382.901	-48.972
5p	9.60	-2.38	0.74	-186.444	-65.987	-310.288	-45.079
5u	9.53	-2.76	0.00	-191.517	-64.729	-329.299	-46.927
5w	9.42	-2.12	0.00	-165.751	-70.621	-309.979	-45.403
5t	9.24	-2.80	0.02	-180.752	-57.365	-314.213	-45.749
5o	9.22	-2.07	0.69	-186.507	-70.523	-295.209	-46.550
5k	8.99	-2.09	0.75	-173.368	-76.333	-276.673	-46.014
5s	8.77	-5.61	0.01	-208.538	-43.152	-385.341	-51.152
4o	8.73	-2.04	1.08	-182.911	-71.973	-270.825	-45.579
4k	8.70	-2.10	1.08	-168.782	-70.834	-245.871	-44.020
5m	8.57	-2.90	0.46	-188.940	-62.079	-321.652	-47.808
4u	8.56	-2.27	0.07	-175.782	-32.925	-288.936	-37.673
5c	8.48	-2.09	0.00	-175.245	-80.278	-290.352	-43.378
4s	8.44	-2.86	0.01	-189.442	-43.940	-327.635	-47.213
5v	8.29	-3.48	0.06	-183.359	-57.420	-336.968	-44.797
4p	8.01	-1.29	2.04	-147.305	-60.879	-193.420	-39.602
5f	7.94	-5.27	0.01	-192.461	-46.186	-350.438	-48.158
4t	7.87	-1.89	0.00	-162.089	-52.020	-277.533	-44.161
5d	7.86	-6.72	0.00	-214.264	-59.131	-375.868	-53.759
5n	7.81	-3.65	0.23	-189.764	-59.266	-318.338	-47.700
5i	7.81	-1.87	0.00	-168.459	-71.542	-293.487	-45.910
5b	7.81	-1.48	0.00	-152.159	-78.140	-267.593	-42.377
5a	7.69	-2.67	0.87	-164.149	-70.229	-255.391	-42.886
4j	7.63	-1.49	1.94	-141.425	-68.416	-207.688	-41.988
4w	7.38	-1.53	0.00	-145.023	-71.624	-240.623	-40.258
5j	7.35	-2.05	0.00	-161.614	-68.986	-277.086	-43.087
4f	7.31	-3.81	0.88	-163.065	-59.071	-270.547	-44.081
4m	7.29	-2.40	0.67	-172.878	-69.816	-279.071	-45.022
5e	7.26	-3.29	0.81	-165.307	-60.333	-252.145	-44.191
4n	7.20	-2.70	0.26	-172.907	-59.020	-282.684	-43.974
4v	7.17	-3.61	1.89	-156.981	-46.920	-264.743	-40.456
4a	7.12	-2.00	1.00	-150.293	-72.677	-219.039	-40.185
4e	7.06	-1.78	0.13	-150.784	-43.595	-239.867	-39.999
4i	6.81	-2.51	1.01	-159.436	-72.202	-255.736	-44.436
5x	6.80	-3.05	0.56	-165.851	-75.414	-302.510	-42.413
4q	6.74	-2.74	0.00	-191.163	-70.123	-311.367	-43.680
5g	6.73	-4.05	0.02	-179.831	-62.972	-318.840	-46.453
5h	6.69	-2.68	0.10	-168.629	-68.265	-284.977	-47.876
4h	6.48	-2.31	0.00	-163.985	-72.555	-264.480	-41.340
4g	6.48	-2.18	0.04	-162.107	-68.993	-273.075	-40.751
4c	6.45	-1.95	0.00	-156.922	-87.434	-238.570	-40.589
4b	6.26	-2.19	0.20	-145.891	-56.856	-237.277	-37.835
4x	6.25	-3.53	0.03	-176.541	-80.563	-267.817	-37.576
TCL	6.18	-1.99	2.55	-142.307	-28.832	-221.306	-39.726
5y	6.01	-2.76	0.00	-148.177	-53.016	-265.272	-32.680
4d	5.68	-6.37	0.00	-197.957	-61.224	-320.810	-50.312
5z	5.54	-3.04	0.00	-144.653	-53.485	-262.111	-32.691
4z	5.00	-1.22	0.78	-112.068	-57.974	-190.243	-30.467
4y	4.91	-1.68	0.04	-127.785	-58.758	-208.272	-27.386

<sup>a</sup> C Score (Consensus Score) integrates a number of popular scoring functions for ranking the affinity of ligands bound to the active site of a receptor and reports the output of total score.

<sup>b</sup> Crash-score revealing the inappropriate penetration into the binding site. Crash scores close to 0 are favorable. Negative numbers indicate penetration.

<sup>c</sup> Polar indicating the contribution of the polar interactions to the total score. The polar score may be useful for excluding docking results that make no hydrogen bonds.

<sup>d</sup> D-score for charge and van der Waals interactions between the protein and the ligand (work of Kuntz) [40].

<sup>e</sup> PMF-score indicating the Helmholtz free energies of interactions for protein-ligand atom pairs (Potential of Mean Force, PMF) (work of Muegge and Martin) [39].

<sup>f</sup> G-score showing hydrogen bonding, complex (ligand–protein), and internal (ligand–ligand) energies (work of Willett's group) [38].

<sup>g</sup> Chem-score points for hydrogen bonding, lipophilic contact, and rotational entropy, along with an intercept term (work of Eldridge, Murray, Auton, Paolini, and Mee) [41].

#### 4.2. General procedure for the synthesis of ethyl aromatic esters (**8a–s**)

Each substituted benzoic acid or aryoxy acetic acid (**7a–s**) 0.088 mol was refluxed for 2–12 h in 2.4 mol of HCl gas saturated anhydrous ethanol. Then a hot solution was poured into 300 mL of water (no hydrochloride separates) to which solid Na<sub>2</sub>CO<sub>3</sub> was added until the solution turns neutral. Precipitated ester was filtered by suction, dried and recrystallized from ethanol or methanol. In case of liquid esters, the neutralized solution was extracted with chloroform (25 mL × 3), the combined extracts were dried over Na<sub>2</sub>SO<sub>4</sub>, filtered, and concentrated under reduced pressure to afford a clear liquid.

#### 4.3. General procedure for the synthesis of acid hydrazides (**9a–s**)

The 0.015 mol of ethyl aromatic esters (**8a–s**) and 0.02 mol of hydrazine hydrate were dissolved in absolute ethanol or methanol (20 mL) to reflux the reaction mixture for 3–6 h for complete hydrazinolysis of ethyl aromatic esters. The product obtained was isolated after cooling as a white or yellow solid and recrystallized from ethanol or methanol.

#### 4.4. General procedure for the preparation of arylsulfonyl hydrazides (**11t–v**)

To a stirred solution of appropriate sulfonyl chloride (0.0025 mol) in dichloromethane (5 mL), a solution of anhydrous hydrazine (0.0125 mol) was added for 2 min and stirred for 15 min and its pH was adjusted to about 11 by adding 10% Na<sub>2</sub>CO<sub>3</sub> solution. The layers were separated and the aqueous phase was extracted with dichloromethane (25 mL × 3). The combined organic layers were dried over MgSO<sub>4</sub>, filtered and the solvent was removed under a reduced pressure at which no further purification of the product was necessary. In case of **11v**, the product obtained in step-

**Table 4**

PLS data summary.

	CoMFA <sup>a</sup>	CoMSIA <sup>a</sup>	CoMFA <sup>b</sup>	CoMSIA <sup>b</sup>	CoMFA <sup>c</sup>	CoMSIA <sup>c</sup>
<i>Statistical parameters</i>						
$q^2$	0.179	0.305	0.341	0.373	0.667	0.599
No. of molecules in training set	52	52	39	39	39	39
No. of molecules in test set	—	—	13	13	13	13
ONC	03	05	03	03	05	06
SEE	0.410	0.304	0.379	0.437	0.244	0.252
$r^2$	0.739	0.865	0.769	0.693	0.922	0.920
$F_{ratio}$	61.941	149.365	89.858	77.136	205.310	205.227
$r_{LOO}^2$	0.788	0.871	0.766	0.689	0.916	0.916
$r_{BS}^2$	0.833	0.955	0.888	0.874	0.981	0.982
S.D.	0.055	0.019	0.034	0.030	0.009	0.011
$r_{pred}^2$	—	—	0.849	0.828	0.896	0.930
<i>Fraction of field contributions</i>						
Steric	0.030	0.023	0.179	0.038	0.211	0.057
Electrostatic	0.074	0.083	0.267	0.109	0.273	0.133
Hydrophobic	—	0.054	—	0.084	—	0.115
Donor	—	0.068	—	0.154	—	0.073
Acceptor	—	0.075	—	0.149	—	0.144

<sup>a</sup>  $q^2$ , square of crossvalidated correlation coefficient; ONC, optimum number of components; SEE, standard error of estimate; S.D., standard deviation;  $r^2$ , square of non-crossvalidated correlation coefficient;  $F$ ,  $r^2/(1 - r^2)$ ;  $r_{BS}^2$ , is mean  $r^2$  of bootstrapping analysis (100 runs); SD<sub>BS</sub>, is mean standard deviation by bootstrapping analysis;  $r_{pred}^2$ , predictive correlation coefficient.

<sup>b</sup> All docked 52 molecules with docked alignment is used in PLS analysis.

<sup>c</sup> The training set of 39 molecules, docked alignment is used in PLS analysis.

<sup>c</sup> The training set of 39 molecules, database alignment is used in PLS analysis.

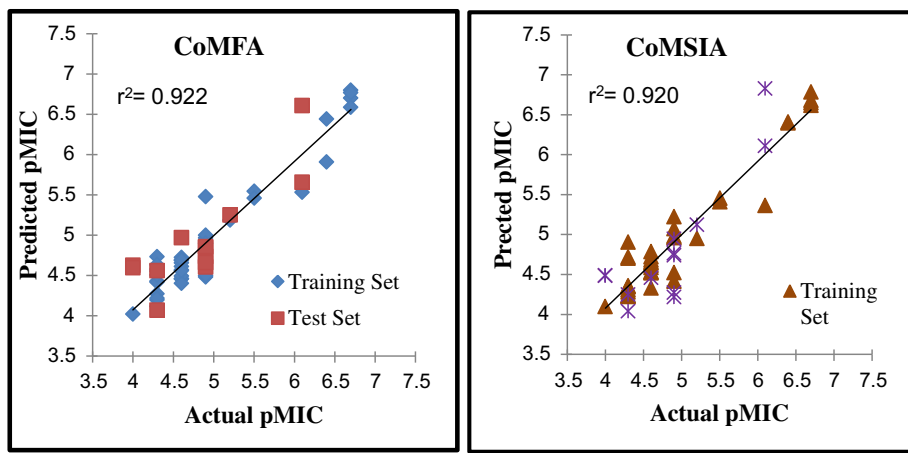


Fig. 7. Scatter plot diagram for CoMFA and CoMSIA analysis by database alignment.

1 i.e., **11u** was hydrolyzed in the presence of 40% NaOH to obtain **11v** as a white crystalline powder.

#### 4.5. Synthesis of 4-(1H-pyrrol-1-yl)-acetophenone (**2**)

A mixture of 2,5-dimethoxytetrahydrofuran (4.23 g, 0.032 mol) and 4-aminoacetophenone (4.05 g, 0.030 mol) in glacial acetic acid (12 mL) was refluxed for 1 h, poured into ice cold water and basified with NaHCO<sub>3</sub> solution. The solid separated was washed with water, dried and recrystallized from ethanol.

(Yield 89%). mp 116–118 °C; FTIR (KBr): 3138, 3002, 2921 (Ar–H), 1676 (C=O) cm<sup>-1</sup>; <sup>1</sup>H NMR (400 MHz, DMSO-*d*<sub>6</sub>) δ ppm: 2.59 (s, 3H, CH<sub>3</sub>), 6.33 (t, 2H, *J* = 2.2, pyrrole–C<sub>3</sub>, C<sub>4</sub>–H), 7.30 (t, 2H, *J* = 2.2, pyrrole–C<sub>2</sub>, C<sub>5</sub>–H), 7.56–7.60 (m, 2H, phenyl–C<sub>3</sub>, C<sub>5</sub>–H), 7.97–8.04 (m, 2H, phenyl–C<sub>2</sub>, C<sub>6</sub>–H); <sup>13</sup>C NMR (100 MHz, DMSO-*d*<sub>6</sub>) δ ppm: 26.43, 111.32, 118.42, 118.84, 129.94, 133.28, 143.14, 196.21; MS (ESI): *m/z* = found 185.11 [M<sup>+</sup>]; calcd. 185.08. Anal. Calcd. for C<sub>12</sub>H<sub>11</sub>NO: C, 77.81; H, 5.99; N, 7.56. Found: C, 77.50; H, 6.01; N, 7.59.

**Table 5**

Actual (Act.) and predicted (Pred) pMIC values and residuals (Δ) of the database aligned training set and test set molecules.

Compd	Act.	CoMFA		CoMSIA		Compd	Act.	CoMFA		CoMSIA	
		Pred.	Δ	Pred.	Δ			Pred.	Δ	Pred.	Δ
<b>4a<sup>a</sup></b>	4.301	4.068	0.233	4.039	0.262	<b>5a</b>	4.000	4.021	-0.021	4.099	-0.099
<b>4b</b>	4.301	4.431	-0.13	4.310	-0.009	<b>5b<sup>a</sup></b>	4.000	4.597	-0.597	4.490	-0.49
<b>4c</b>	4.903	4.481	0.422	4.417	0.486	<b>5c</b>	4.301	4.577	-0.276	4.703	-0.402
<b>4d</b>	4.602	4.459	0.143	4.527	0.075	<b>5d</b>	4.602	4.657	-0.055	4.645	-0.043
<b>4e</b>	4.301	4.418	-0.117	4.236	0.065	<b>5e</b>	4.602	4.690	-0.088	4.536	0.066
<b>4f</b>	4.301	4.555	-0.254	4.359	-0.058	<b>5f</b>	4.602	4.725	-0.123	4.586	0.016
<b>4g</b>	4.301	4.198	0.103	4.349	-0.048	<b>5g</b>	4.602	4.493	0.109	4.614	-0.012
<b>4h</b>	4.301	4.273	0.028	4.345	-0.044	<b>5h</b>	4.602	4.402	0.2	4.654	-0.052
<b>4i</b>	4.602	4.569	0.033	4.520	0.082	<b>5i<sup>a</sup></b>	4.903	4.856	0.047	4.764	0.139
<b>4j<sup>a</sup></b>	4.903	4.735	0.168	4.272	0.631	<b>5j</b>	4.602	4.559	0.043	4.722	-0.12
<b>4k</b>	4.903	4.967	-0.064	4.978	-0.075	<b>5k</b>	6.097	5.534	0.563	5.364	0.733
<b>4l</b>	4.903	5.000	-0.097	5.072	-0.169	<b>5l</b>	5.505	5.544	-0.039	5.456	0.049
<b>4m<sup>a</sup></b>	4.903	4.606	0.297	4.740	0.163	<b>5m</b>	5.505	5.461	0.044	5.408	0.097
<b>4n</b>	4.301	4.733	-0.432	4.720	-0.419	<b>5n<sup>a</sup></b>	5.204	5.250	-0.046	5.123	0.081
<b>4o</b>	4.602	4.457	0.145	4.681	-0.079	<b>5o</b>	4.301	4.632	-0.331	4.904	-0.603
<b>4p</b>	4.602	4.611	-0.009	4.331	0.271	<b>5p</b>	4.602	4.692	-0.09	4.787	-0.185
<b>4q</b>	4.301	4.118	0.183	4.283	0.018	<b>5q</b>	4.903	4.499	0.404	4.524	0.379
<b>4r</b>	6.398	6.443	-0.045	6.409	-0.011	<b>5r</b>	6.699	6.799	-0.1	6.618	0.081
<b>4s</b>	6.699	6.704	-0.005	6.680	0.019	<b>5s</b>	6.699	6.769	-0.07	6.785	-0.086
<b>4t<sup>a</sup></b>	6.097	5.656	0.441	6.109	-0.012	<b>5t</b>	6.398	5.908	0.49	6.396	0.002
<b>4u</b>	6.699	6.588	0.111	6.651	0.048	<b>5u<sup>a</sup></b>	6.097	6.608	-0.511	6.828	-0.731
<b>4v</b>	5.204	5.187	0.017	4.951	0.253	<b>5v</b>	4.903	5.479	-0.576	5.224	-0.321
<b>4w<sup>a</sup></b>	4.903	4.660	0.243	4.217	0.686	<b>5w<sup>a</sup></b>	4.602	4.969	-0.367	4.459	0.143
<b>4x<sup>a</sup></b>	4.903	4.849	0.054	4.946	-0.043	<b>5x</b>	4.903	4.900	0.003	4.959	-0.056
<b>4y</b>	4.301	4.219	0.082	4.230	0.071	<b>5y<sup>a</sup></b>	4.301	4.559	-0.258	4.248	0.053
<b>4z<sup>a</sup></b>	4.000	4.627	-0.627	4.482	-0.482	<b>5z</b>	4.301	4.507	-0.206	4.224	0.077

<sup>a</sup> Indicates test set compounds.

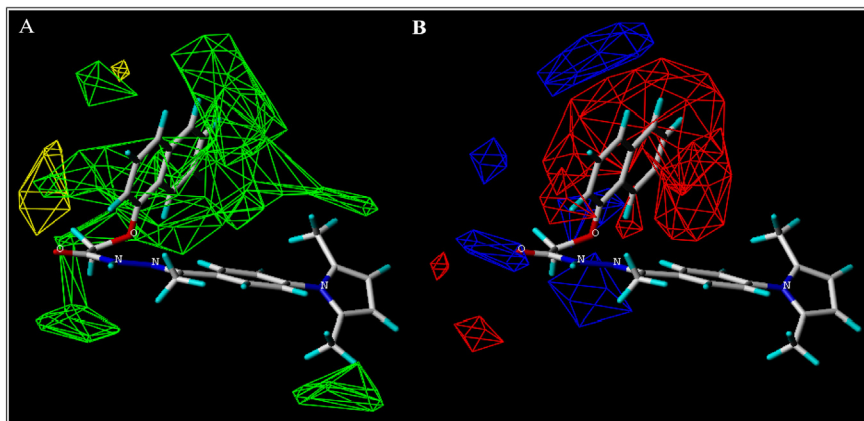


**Fig. 8.** CoMFA Stdev\*Coeff (A) steric and (B) electrostatic contour maps. The most active molecule **5r** is displayed in the background (database alignment).

#### 4.7. General procedure for the synthesis of pyrrole hydrazones (**4a**–**z** and **5a**–**z**)

An ethanolic solution of 4-(1*H*-pyrrol-1-yl)-acetophenone (**2**) (0.93 g, 0.005 mol) or 4-(2,5-dimethyl-1*H*-pyrrol-1-yl)-acetophenone (**3**) (1.07 g, 0.005 mol) was added to a hot ethanolic solution of hydrazides (0.005 mol) in the presence of catalytic amount of acetic acid and the mixture was heated under reflux for 2–4 h and then cooled in an ice bath. The yellow or brown flakes separated were filtered, washed repeatedly with ethanol, dried in vacuum and purified using column chromatography (ethyl acetate:petroleum ether; 6:4) to afford the final compound.

*In case of hydrazine hydrochloride:* Phenyl hydrazine hydrochloride or semicarbazide hydrochloride (0.87 g or 0.7 g, 0.006 mol) and NaHCO<sub>3</sub> (0.5 g, 0.006 mol) were added to a solution of ketone **2** or **3** (0.005 mol) in ethanol (15 mL). The mixture was stirred for 1 h, to which trifluoroacetic acid (~25 mg, ~0.1%) was added and stirred for 2 h. The precipitated solid was collected under suction filtration and dried, followed by recrystallization in aqueous methanol, giving the hydrazones (**4w**–**x** and **5w**–**x**) in varying yields.

##### 4.7.1. *N'*-(1-(4-(1*H*-Pyrrol-1-yl)phenyl)ethylidene)isonicotinohydrazide (**4a**)

(Yield 70%). mp 255–257 °C; FTIR (KBr): 3236 (NH), 3142, 3025 (Ar–H), 1648 (C=O), 1606 (C=N) cm<sup>−1</sup>; <sup>1</sup>H NMR (400 MHz, DMSO-*d*<sub>6</sub>) δ ppm: 2.42 (s, 3H, CH<sub>3</sub>), 6.30 (s, 2H, pyrrole–C<sub>3</sub>, C<sub>4</sub>–H), 7.29 (s, 2H, pyrrole–C<sub>2</sub>, C<sub>5</sub>–H), 7.56 (d, 2H, *J* = 8.5, phenyl–C<sub>3</sub>, C<sub>5</sub>–H), 7.83 (d, 2H, *J* = 5.3, pyridine–C<sub>2</sub>, C<sub>6</sub>–H), 7.97 (d, 2H, *J* = 8.6, phenyl–C<sub>2</sub>, C<sub>6</sub>–H), 8.76 (d, 2H, *J* = 5.3, pyridine–C<sub>3</sub>, C<sub>5</sub>–H), 11.04 (s, 1H, NH); <sup>13</sup>C NMR (75 MHz, DMSO-*d*<sub>6</sub>) δ ppm: 15.13, 111.34, 119.19, 119.36, 122.33, 128.43, 134.91, 141.23, 141.61, 151.59, 156.70, 156.70, 162.86; MS (ESI): *m/z* = found 305.14 [M<sup>+</sup> + 1], 306.14 [M<sup>+</sup> + 2]; calcd. 304.13. Anal. Calcd. for C<sub>18</sub>H<sub>16</sub>N<sub>4</sub>O: C, 71.04; H, 5.30; N, 18.41. Found: C, 70.75; H, 5.32; N, 18.33.

##### 4.7.2. *N'*-(1-(4-(1*H*-Pyrrol-1-yl)phenyl)ethylidene)nicotinohydrazide (**4b**)

(Yield 72%). mp 235–237 °C; FTIR (KBr): 3215 (NH), 3028, 2925 (Ar–H), 1649 (C=O), 1603 (C=N) cm<sup>−1</sup>; <sup>1</sup>H NMR (400 MHz, DMSO-*d*<sub>6</sub>) δ ppm: 2.42 (s, 3H, CH<sub>3</sub>), 6.31 (s, 2H, pyrrole–C<sub>3</sub>, C<sub>4</sub>–H), 7.33 (s, 2H, pyrrole–C<sub>2</sub>, C<sub>5</sub>–H), 7.59 (d, 2H, *J* = 7.4, phenyl–C<sub>3</sub>, C<sub>5</sub>–H), 7.66 (s, 1H, pyridine–C<sub>5</sub>–H), 7.96 (d, 2H, *J* = 7.5, phenyl–C<sub>2</sub>, C<sub>6</sub>–H), 8.24–9.07 (m, 3H, pyridine–C<sub>2</sub>, C<sub>4</sub>, C<sub>6</sub>–H), 10.99 (s, 1H, NH); <sup>13</sup>C NMR (100 MHz, DMSO-*d*<sub>6</sub>) δ ppm: 16.75, 110.71, 118.67, 127.51, 129.53, 129.88, 130.77, 135.30, 134.49, 143.11, 148.81, 149.19, 160.58, 174.54; MS (ESI): *m/z*

*z* = found 304.33 [M<sup>+</sup>]; calcd. 304.13. Anal. Calcd. for C<sub>18</sub>H<sub>16</sub>N<sub>4</sub>O: C, 71.04; H, 5.3; N, 18.41. Found: C, 71.32; H, 5.27; N, 18.33.

##### 4.7.3. *N'*-(1-(4-(1*H*-Pyrrol-1-yl)phenyl)ethylidene)-4-(1*H*-pyrrol-1-yl)benzohydrazide (**4c**)

(Yield 63%). mp 288–290 °C; FTIR (KBr): 3327 (NH), 3144, 2923, 2855 (Ar–H), 1661 (C=O), 1607 (C=N) cm<sup>−1</sup>; <sup>1</sup>H NMR (400 MHz, DMSO-*d*<sub>6</sub>) δ ppm: 2.42 (s, 3H, CH<sub>3</sub>), 6.29 (s, 2H, pyrrole–C<sub>3</sub>, C<sub>4</sub>–H), 6.32 (t, 2H, *J* = 2.1, hydrazide–pyrrole–C<sub>3</sub>, C<sub>4</sub>–H), 7.31 (s, 2H, pyrrole–C<sub>2</sub>, C<sub>5</sub>–H), 7.37 (t, 2H, *J* = 2.2, hydrazide–pyrrole–C<sub>2</sub>, C<sub>5</sub>–H), 7.55–8.01 (m, 8H, phenyl–C<sub>2</sub>, C<sub>3</sub>, C<sub>5</sub>, C<sub>6</sub>–H and hydrazide–phenyl–C<sub>2</sub>, C<sub>3</sub>, C<sub>5</sub>, C<sub>6</sub>–H), 10.80 (s, 1H, NH); <sup>13</sup>C NMR (100 MHz, DMSO-*d*<sub>6</sub>) δ ppm: 14.23, 110.63, 110.82, 118.66, 118.86, 119.00, 128.09, 129.14, 129.66, 129.85, 133.31, 143.29, 143.35, 148.11, 163.70; MS (ESI): *m/z* = found 368.31 [M<sup>+</sup>]; calcd. 368.16. Anal. Calcd. for C<sub>23</sub>H<sub>20</sub>N<sub>4</sub>O: C, 74.98; H, 5.47; N, 15.21. Found: C, 75.27; H, 5.44; N, 15.27.

##### 4.7.4. *N'*-(1-(4-(1*H*-Pyrrol-1-yl)phenyl)ethylidene)-4-(2,5-dimethyl-1*H*-pyrrol-1-yl)benzohydrazide (**4d**)

(Yield 67%). mp 228–230 °C; FTIR (KBr): 3325 (NH), 3135, 2922 (Ar–H), 1652 (C=O), 1605 (C=N) cm<sup>−1</sup>; <sup>1</sup>H NMR (400 MHz, DMSO-*d*<sub>6</sub>) δ ppm: 2.02 (s, 6H, 2CH<sub>3</sub>), 2.41 (s, 3H, CH<sub>3</sub>), 5.85 (s, 2H, dimethylpyrrole–C<sub>3</sub>, C<sub>4</sub>–H), 6.30 (s, 2H, pyrrole–C<sub>3</sub>, C<sub>4</sub>–H), 7.40–7.45 (m, 4H, pyrrole–C<sub>2</sub>, C<sub>5</sub>–H and phenyl–C<sub>3</sub>, C<sub>5</sub>–H), 7.67 (d, 2H, *J* = 6.6, hydrazide–phenyl–C<sub>3</sub>, C<sub>5</sub>–H), 7.94–8.02 (m, 4H, phenyl–C<sub>2</sub>, C<sub>6</sub>–H and hydrazide–phenyl–C<sub>2</sub>, C<sub>6</sub>–H), 10.80 (s, 1H, NH); <sup>13</sup>C NMR (75 MHz, DMSO-*d*<sub>6</sub>) δ ppm: 12.56, 13.40, 106.92, 111.31, 119.18, 119.36, 128.04, 128.26, 129.30, 129.65, 135.17, 141.38, 142.03, 145.60, 162.29; MS (ESI): *m/z* = found 396.35 [M<sup>+</sup>]; calcd. 396.20. Anal. Calcd. for C<sub>25</sub>H<sub>24</sub>N<sub>4</sub>O: C, 75.73; H, 6.10; N, 14.13. Found: C, 75.42; H, 6.12; N, 14.18.

##### 4.7.5. *N'*-(1-(4-(1*H*-Pyrrol-1-yl)phenyl)ethylidene)benzohydrazide (**4e**)

(Yield 77%). mp 253–255 °C; FTIR (KBr): 3192 (NH), 3000 (Ar–H), 1644 (C=O), 1609 (C=N) cm<sup>−1</sup>; <sup>1</sup>H NMR (400 MHz, DMSO-*d*<sub>6</sub>) δ ppm: 2.41 (s, 3H, CH<sub>3</sub>), 6.29 (s, 2H, pyrrole–C<sub>3</sub>, C<sub>4</sub>–H), 7.26 (s, 2H, pyrrole–C<sub>2</sub>, C<sub>5</sub>–H), 7.47–7.55 (m, 5H, hydrazide–phenyl–C<sub>3</sub>, C<sub>4</sub>, C<sub>5</sub>–H and phenyl–C<sub>3</sub>, C<sub>5</sub>–H), 7.90–7.94 (m, 4H, phenyl–C<sub>2</sub>, C<sub>6</sub>–H and hydrazide–phenyl–C<sub>2</sub>, C<sub>6</sub>–H), 10.73 (s, 1H, NH); <sup>13</sup>C NMR (100 MHz, DMSO-*d*<sub>6</sub>) δ ppm: 16.90, 110.69, 118.68, 127.73, 128.79, 129.93, 131.37, 131.93, 134.73, 140.66, 147.90, 164.33; MS (ESI): *m/z* = found 304.14 [M<sup>+</sup> + 1], 305.15 [M<sup>+</sup> + 2]; calcd. 303.14. Anal. Calcd. for C<sub>19</sub>H<sub>17</sub>N<sub>3</sub>O: C, 75.23; H, 5.65; N, 13.85. Found: C, 74.92; H, 5.67; N, 13.79.

**4.7.6. *N'*-(1-(4-(1*H*-Pyrrol-1-yl)phenyl)ethylidene)-4-methylbenzohydrazide (**4f**)**

(Yield 73%). mp 264–266 °C; FTIR (KBr): 3234 (NH), 2998, 2920, 2859 (Ar—H), 1649 (C=O), 1608 (C=N) cm<sup>−1</sup>; <sup>1</sup>H NMR (400 MHz, DMSO-*d*<sub>6</sub>) δ ppm: 2.39 (s, 3H, CH<sub>3</sub>), 2.40 (s, 3H, phenyl—CH<sub>3</sub>), 6.29 (s, 2H, pyrrole—C<sub>3</sub>, C<sub>4</sub>—H), 7.31 (d, 2H, *J* = 7.9, hydrazide—phenyl—C<sub>3</sub>, C<sub>5</sub>—H), 7.35 (s, 2H, pyrrole—C<sub>2</sub>, C<sub>5</sub>—H), 7.59 (d, 2H, *J* = 7.7, phenyl—C<sub>3</sub>, C<sub>5</sub>—H), 7.80 (s, 2H, phenyl—C<sub>2</sub>, C<sub>6</sub>—H), 7.92 (s, 2H, hydrazide—phenyl—C<sub>2</sub>, C<sub>6</sub>—H), 10.68 (s, 1H, NH); <sup>13</sup>C NMR (100 MHz, DMSO-*d*<sub>6</sub>) δ ppm: 16.81, 21.50, 110.65, 118.61, 118.69, 127.69, 129.50, 130.21, 134.81, 140.37, 143.11, 149.37, 164.33; MS (ESI): *m/z* = found 317.36 [M<sup>+</sup>]; calcd. 317.15. Anal. Calcd. for C<sub>20</sub>H<sub>19</sub>N<sub>3</sub>O: C, 75.69; H, 6.03; N, 13.24. Found: C, 75.99; H, 6.01; N, 13.18.

**4.7.7. *N'*-(1-(4-(1*H*-Pyrrol-1-yl)phenyl)ethylidene)-4-chlorobenzohydrazide (**4g**)**

(Yield 69%). mp 210–212 °C; FTIR (KBr): 3270 (NH), 3048, 2922, 2852 (Ar—H), 1653 (C=O), 1606 (C=N), 721 (C—Cl) cm<sup>−1</sup>; <sup>1</sup>H NMR (400 MHz, DMSO-*d*<sub>6</sub>) δ ppm: 2.31 (s, 3H, CH<sub>3</sub>), 6.27 (t, 2H, *J* = 2.0, pyrrole—C<sub>3</sub>, C<sub>4</sub>—H), 7.27 (t, 2H, *J* = 2.0, pyrrole—C<sub>2</sub>, C<sub>5</sub>—H), 7.41 (d, 2H, *J* = 8.7, phenyl—C<sub>3</sub>, C<sub>5</sub>—H), 7.60 (d, 2H, *J* = 8.7, 4-chlorophenyl—C<sub>3</sub>, C<sub>5</sub>—H), 7.78 (d, 2H, *J* = 8.6, phenyl—C<sub>2</sub>, C<sub>6</sub>—H), 7.91 (d, 2H, *J* = 8.7, 4-chlorophenyl—C<sub>3</sub>, C<sub>5</sub>—H), 10.82 (s, 1H, NH); <sup>13</sup>C NMR (100 MHz, DMSO-*d*<sub>6</sub>) δ ppm: 14.38, 110.82, 119.56, 127.33, 128.51, 128.77, 129.27, 130.01, 133.30, 135.22, 140.11, 145.29, 160.28; MS (ESI): *m/z* = found 337.52 [M<sup>+</sup>], 339.34 [M<sup>+</sup>+2]; calcd. 337.10. Anal. Calcd. for C<sub>19</sub>H<sub>16</sub>ClN<sub>3</sub>O: C, 67.56; H, 4.77; N, 12.44. Found: C, 67.83; H, 4.75; N, 12.39.

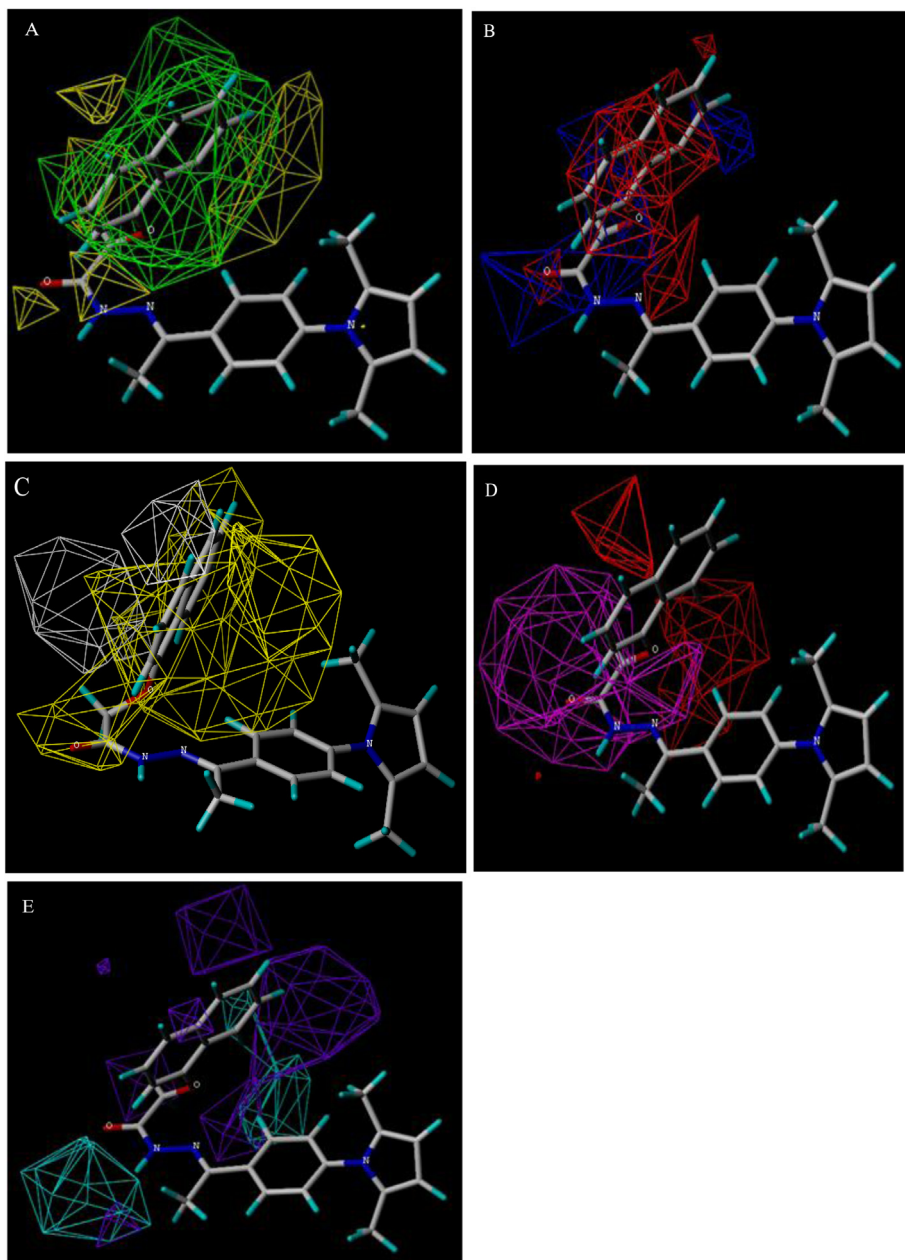


**Fig. 9.** Stdev\*coeff contour maps of CoMSIA analysis for compound **5r** by database alignment. (A) Steric contour map. Green and yellow contours refer to sterically favored and disfavored regions, respectively. (B) Electrostatic contour map. Blue and red contours refer to regions where electron-donating and electron-withdrawing groups are favored, respectively. (C) Hydrophobic contour map. White contours (20% contribution) refer to regions where hydrophilic substituents are favored; yellow contours (80% contribution) indicate regions where hydrophobic substituents are favored. (D) Hydrogen bond acceptor contour map. The magenta contours (80%) for hydrogen bond acceptor group increase activity, red contours (20%) indicate the disfavored region. (E) Hydrogen bond donor contour map. The cyan and purple (80% and 20% contributions) contours indicate favorable and unfavorable hydrogen bond donor groups, respectively. (For interpretation of the references to color in this figure legend, the reader is referred to the web version of this article.)

#### 4.7.8. *N'*-(1-(4-(1*H*-Pyrrol-1-yl)phenyl)ethylidene)-4-bromobenzohydrazide (**4h**)

(Yield 66%). mp 209–210 °C; FTIR (KBr): 3202 (NH), 3042, 2919, 2849 (Ar–H), 1647 (C=O), 1606 (C=N), 722 (C–Br) cm<sup>−1</sup>; <sup>1</sup>H NMR (400 MHz, DMSO-*d*<sub>6</sub>) δ ppm: 2.35 (s, 3H, CH<sub>3</sub>), 6.25 (t, 2H, *J* = 2.1, pyrrole–C<sub>3</sub>, C<sub>4</sub>–H), 7.26 (t, 2H, *J* = 2.0, pyrrole–C<sub>2</sub>, C<sub>5</sub>–H), 7.43–7.57 (m, 2H, phenyl–C<sub>3</sub>, C<sub>5</sub>–H), 7.62 (d, 2H, *J* = 8.7, 4-bromophenyl–C<sub>3</sub>, C<sub>5</sub>–H), 7.77–7.85 (m, 2H, phenyl–C<sub>2</sub>, C<sub>6</sub>–H), 7.90 (d, 2H, *J* = 8.7, 4-bromophenyl–C<sub>3</sub>, C<sub>5</sub>–H), 10.85 (s, 1H, NH); <sup>13</sup>C NMR (100 MHz, DMSO-*d*<sub>6</sub>) δ ppm: 14.31, 110.80, 119.31, 126.80, 127.57, 128.63, 129.11, 130.89, 131.28, 134.09, 141.03, 145.71, 162.20; MS (ESI): *m/z* = found 381.33 [M<sup>+</sup>]; 383.39 [M<sup>+</sup>+2]; calcd. 381.05. Anal. Calcd. for C<sub>19</sub>H<sub>16</sub>BrN<sub>3</sub>O: C, 59.70; H, 4.22; N, 10.99. Found: C, 59.93; H, 4.20; N, 10.95.

#### 4.7.9. *N'*-(1-(4-(1*H*-Pyrrol-1-yl)phenyl)ethylidene)-2-chlorobenzohydrazide (**4i**)

(Yield 67%). mp 213–215 °C; FTIR (KBr): 3289 (NH), 3044, 2924 (Ar–H), 1650 (C=O), 1605 (C=N), 726 (C–Cl) cm<sup>−1</sup>; <sup>1</sup>H NMR (400 MHz, DMSO-*d*<sub>6</sub>) δ ppm: 2.34 (s, 3H, CH<sub>3</sub>), 6.26 (t, 2H, *J* = 2.1, pyrrole–C<sub>3</sub>, C<sub>4</sub>–H), 7.27 (t, 2H, *J* = 2.0, pyrrole–C<sub>2</sub>, C<sub>5</sub>–H), 7.41–7.66 (m, 4H, 2-chlorophenyl–C<sub>5</sub>, C<sub>6</sub>–H and phenyl–C<sub>3</sub>, C<sub>5</sub>–H), 7.70–7.78 (m, 2H, 2-chlorophenyl–C<sub>3</sub>, C<sub>4</sub>–H), 7.85–7.90 (m, 2H, phenyl–C<sub>2</sub>, C<sub>6</sub>–H), 10.89 (s, 1H, NH); <sup>13</sup>C NMR (100 MHz, DMSO-*d*<sub>6</sub>) δ ppm: 14.20, 110.82, 120.11, 126.89, 128.83, 129.35, 129.78, 130.09, 131.88, 133.05, 134.29, 134.60, 142.01, 145.38, 162.39; MS (ESI): *m/z* = found 337.28 [M<sup>+</sup>], 339.51 [M<sup>+</sup>+2]; calcd. 337.10. Anal. Calcd. for C<sub>19</sub>H<sub>16</sub>ClN<sub>3</sub>O: C, 67.56; H, 4.77; N, 12.44. Found: C, 67.83; H, 4.75; N, 12.48.

#### 4.7.10. *N'*-(1-(4-(1*H*-Pyrrol-1-yl)phenyl)ethylidene)-4-hydroxybenzohydrazide (**4j**)

(Yield 63%). mp 283–285 °C; FTIR (KBr): 3441 (OH), 3281 (NH), 3032, 2923 (Ar–H), 1657 (C=O), 1606 (C=N) cm<sup>−1</sup>; <sup>1</sup>H NMR (400 MHz, DMSO-*d*<sub>6</sub>) δ ppm: 2.35 (s, 3H, CH<sub>3</sub>), 5.32 (s, 1H, OH), 6.29 (t, 2H, *J* = 2.0, pyrrole–C<sub>3</sub>, C<sub>4</sub>–H), 6.85–6.93 (m, 2H, 4-hydroxyphenyl–C<sub>3</sub>, C<sub>5</sub>–H), 7.27 (t, 2H, *J* = 2.0, pyrrole–C<sub>2</sub>, C<sub>5</sub>–H), 7.50 (d, 2H, *J* = 8.6, phenyl–C<sub>3</sub>, C<sub>5</sub>–H), 7.69–7.88 (m, 4H, phenyl–C<sub>2</sub>, C<sub>6</sub>–H and 4-hydroxyphenyl–C<sub>2</sub>, C<sub>6</sub>–H), 10.87 (s, 1H, NH); <sup>13</sup>C NMR (100 MHz, DMSO-*d*<sub>6</sub>) δ ppm: 14.29, 110.83, 116.09, 119.33, 125.39, 128.35, 129.30, 129.77, 132.35, 141.03, 145.23, 161.89, 162.73; MS (ESI): *m/z* = found 319.54 [M<sup>+</sup>]; calcd. 319.13. Anal. Calcd. for C<sub>19</sub>H<sub>17</sub>N<sub>3</sub>O<sub>2</sub>: C, 71.46; H, 5.37; N, 13.16. Found: C, 71.17; H, 5.39; N, 13.21.

#### 4.7.11. *N'*-(1-(4-(1*H*-Pyrrol-1-yl)phenyl)ethylidene)-2-phenoxyacetohydrazide (**4k**)

(Yield 75%). mp 193–195 °C; FTIR (KBr): 3176 (NH), 3048, 2829 (Ar–H), 1648 (C=O), 1591 (C=N), 1287 (C–O–C) cm<sup>−1</sup>; <sup>1</sup>H NMR (400 MHz, DMSO-*d*<sub>6</sub>) δ ppm: 2.33 (s, 3H, CH<sub>3</sub>), 5.18 (s, 2H, OCH<sub>2</sub>), 6.27 (t, 2H, *J* = 2.1, pyrrole–C<sub>3</sub>, C<sub>4</sub>–H), 6.90–7.03 (m, 3H, phenoxy–C<sub>2</sub>, C<sub>4</sub>, C<sub>6</sub>–H), 7.24 (t, 2H, *J* = 2.0, pyrrole–C<sub>2</sub>, C<sub>5</sub>–H), 7.27–7.31 (m, 2H, phenoxy–C<sub>3</sub>, C<sub>5</sub>–H), 7.53 (d, 2H, *J* = 8.7, phenyl–C<sub>3</sub>, C<sub>5</sub>–H), 7.89 (d, 2H, *J* = 8.7, phenyl–C<sub>2</sub>, C<sub>6</sub>–H), 10.89 (s, 1H, NH); <sup>13</sup>C NMR (100 MHz, DMSO-*d*<sub>6</sub>) δ ppm: 13.39, 65.33, 110.80, 114.29, 119.93, 121.03, 128.89, 129.39, 129.85, 133.88, 142.35, 145.73, 157.39, 169.83; MS (ESI): *m/z* = found 333.21 [M<sup>+</sup>]; calcd. 333.15. Anal. Calcd. for C<sub>20</sub>H<sub>19</sub>N<sub>3</sub>O<sub>2</sub>: C, 72.05; H, 5.74; N, 12.60. Found: C, 71.76; H, 5.76; N, 12.55.

#### 4.7.12. *N'*-(1-(4-(1*H*-Pyrrol-1-yl)phenyl)ethylidene)-2-(*p*-tolyloxy)acetohydrazide (**4l**)

(Yield 70%). mp 205–207 °C; FTIR (KBr): 3178 (NH), 3051 (Ar–H), 1649 (C=O), 1589 (C=N), 1288 (C–O–C) cm<sup>−1</sup>; <sup>1</sup>H NMR (400 MHz, DMSO-*d*<sub>6</sub>) δ ppm: 2.32 (s, 3H, CH<sub>3</sub>), 2.39 (s, 3H, phenoxy–CH<sub>3</sub>), 5.13 (s, 2H, OCH<sub>2</sub>), 6.29 (t, 2H, *J* = 2.0, pyrrole–C<sub>3</sub>, C<sub>4</sub>–

H), 6.89–7.11 (m, 4H, phenoxy–C<sub>2</sub>, C<sub>3</sub>, C<sub>5</sub>, C<sub>6</sub>–H), 7.25 (t, 2H, *J* = 2.0, pyrrole–C<sub>2</sub>, C<sub>5</sub>–H), 7.52 (m, 2H, phenyl–C<sub>3</sub>, C<sub>5</sub>–H), 7.91 (m, 2H, phenyl–C<sub>2</sub>, C<sub>6</sub>–H), 10.88 (s, 1H, NH); <sup>13</sup>C NMR (100 MHz, DMSO-*d*<sub>6</sub>) δ ppm: 13.35, 21.29, 65.39, 110.82, 114.20, 119.90, 129.29, 129.80, 130.03, 130.63, 133.89, 141.78, 146.00, 156.29, 169.73; MS (ESI): *m/z* = found 347.45 [M<sup>+</sup>]; calcd. 347.16. Anal. Calcd. for C<sub>21</sub>H<sub>21</sub>N<sub>3</sub>O<sub>2</sub>: C, 72.60; H, 6.09; N, 12.10; O, 9.21. Found: C, 72.89; H, 6.07; N, 12.14.

#### 4.7.13. *N'*-(1-(4-(1*H*-Pyrrol-1-yl)phenyl)ethylidene)-2-(4-chlorophenoxy)acetohydrazide (**4m**)

(Yield 70%). mp 197–199 °C; FTIR (KBr): 3187 (NH), 3107, 2917 (Ar–H), 1688 (C=O), 1611 (C=N), 1267 (C–O–C), 714 (C–Cl) cm<sup>−1</sup>; <sup>1</sup>H NMR (400 MHz, DMSO-*d*<sub>6</sub>) δ ppm: 2.30 (s, 3H, CH<sub>3</sub>), 5.16 (s, 2H, OCH<sub>2</sub>), 6.29 (t, 2H, *J* = 2.0, pyrrole–C<sub>3</sub>, C<sub>4</sub>–H), 7.00 (dd, 2H, *J* = 8.8, phenoxy–C<sub>2</sub>, C<sub>6</sub>–H), 7.25 (t, 2H, *J* = 2.0, pyrrole–C<sub>2</sub>, C<sub>5</sub>–H), 7.26–7.29 (m, 2H, phenoxy–C<sub>3</sub>, C<sub>5</sub>–H), 7.51 (d, 2H, *J* = 8.7, phenyl–C<sub>3</sub>, C<sub>5</sub>–H), 7.90 (dd, 2H, *J* = 8.5, phenyl–C<sub>2</sub>, C<sub>6</sub>–H), 10.86 (s, 1H, NH); <sup>13</sup>C NMR (100 MHz, DMSO-*d*<sub>6</sub>) δ ppm: 17.02, 65.40, 110.67, 116.05, 118.67, 118.78, 127.38, 128.91, 129.30, 130.90, 133.22, 140.29, 147.54, 157.00, 169.45; MS (ESI): *m/z* = found 368.11 [M<sup>+</sup> + 1], 370.11 [M<sup>+</sup> + 2]; calcd. 367.11. Anal. Calcd. for C<sub>20</sub>H<sub>18</sub>ClN<sub>3</sub>O<sub>2</sub>: C, 65.31; H, 4.93; N, 11.42. Found: C, 65.05; H, 4.95; N, 11.47.

#### 4.7.14. *N'*-(1-(4-(1*H*-Pyrrol-1-yl)phenyl)ethylidene)-2-(4-bromophenoxy)acetohydrazide (**4n**)

(Yield 71%). mp 186–188 °C; FTIR (KBr): 3186 (NH), 3099, 2924, 2858 (Ar–H), 1687 (C=O), 1620 (C=N), 1280 (C–O–C), 714 (C–Br) cm<sup>−1</sup>; <sup>1</sup>H NMR (400 MHz, DMSO-*d*<sub>6</sub>) δ ppm: 2.36 (s, 3H, CH<sub>3</sub>), 5.15 (s, 2H, OCH<sub>2</sub>), 6.31 (t, 2H, *J* = 2.0, pyrrole–C<sub>3</sub>, C<sub>4</sub>–H), 6.86–6.95 (m, 2H, phenoxy–C<sub>2</sub>, C<sub>6</sub>–H), 7.20 (t, 2H, *J* = 2.0, pyrrole–C<sub>2</sub>, C<sub>5</sub>–H), 7.37–7.42 (m, 2H, phenoxy–C<sub>3</sub>, C<sub>5</sub>–H), 7.48 (d, 2H, *J* = 8.7, phenyl–C<sub>3</sub>, C<sub>5</sub>–H), 7.84 (d, 2H, *J* = 8.6, phenyl–C<sub>2</sub>, C<sub>6</sub>–H), 10.80 (s, 1H, NH); <sup>13</sup>C NMR (100 MHz, DMSO-*d*<sub>6</sub>) δ ppm: 13.33, 65.81, 110.65, 116.55, 118.62, 118.80, 127.35, 129.43, 129.80, 131.79, 134.86, 141.82, 145.89, 156.92, 169.40; MS (ESI): *m/z* = found 412.06 [M<sup>+</sup> + 1], 414.06 [M<sup>+</sup> + 3]; calcd. 411.06. Anal. Calcd. for C<sub>20</sub>H<sub>18</sub>BrN<sub>3</sub>O<sub>2</sub>: C, 58.26; H, 4.40; N, 10.19. Found: C, 58.03; H, 4.42; N, 10.15.

#### 4.7.15. *N'*-(1-(4-(1*H*-Pyrrol-1-yl)phenyl)ethylidene)-2-(2-chlorophenoxy)acetohydrazide (**4o**)

(Yield 69%). mp 181–183 °C; FTIR (KBr): 3192 (NH), 3113, 2924 (Ar–H), 1704 (C=O), 1606 (C=N), 1254 (C–O–C), 712 (C–Cl) cm<sup>−1</sup>; <sup>1</sup>H NMR (400 MHz, DMSO-*d*<sub>6</sub>) δ ppm: 2.35 (s, 3H, CH<sub>3</sub>), 5.28 (s, 2H, OCH<sub>2</sub>), 6.28 (t, 2H, *J* = 2.1, pyrrole–C<sub>3</sub>, C<sub>4</sub>–H), 6.93–6.96 (m, 2H, phenoxy–C<sub>4</sub>, C<sub>6</sub>–H), 7.23 (m, 1H, phenoxy–C<sub>5</sub>–H), 7.28 (t, 2H, *J* = 2.0, pyrrole–C<sub>2</sub>, C<sub>5</sub>–H), 7.37–7.39 (m, 1H, phenoxy–C<sub>3</sub>–H), 7.51–7.55 (m, 2H, phenyl–C<sub>3</sub>, C<sub>5</sub>–H), 7.85–7.89 (m, 2H, phenyl–C<sub>2</sub>, C<sub>6</sub>–H), 10.90 (s, 1H, NH); <sup>13</sup>C NMR (100 MHz, DMSO-*d*<sub>6</sub>) δ ppm: 13.38, 65.80, 110.66, 113.54, 113.74, 118.67, 118.78, 121.34, 127.39, 127.74, 129.83, 134.47, 134.60, 140.30, 147.58, 153.63, 169.17; MS (ESI): *m/z* = found 367.81 [M<sup>+</sup>], 365.44 [M<sup>+</sup> − 2]; calcd. 367.11. Anal. Calcd. for C<sub>20</sub>H<sub>18</sub>ClN<sub>3</sub>O<sub>2</sub>: C, 65.31; H, 4.93; N, 11.42. Found: C, 65.57; H, 4.91; N, 11.37.

#### 4.7.16. *N'*-(1-(4-(1*H*-Pyrrol-1-yl)phenyl)ethylidene)-2-(4-hydroxyphenoxy)acetohydrazide (**4p**)

(Yield 63%). mp 289–291 °C; FTIR (KBr): 3436 (OH), 3268 (NH), 3049, 2923 (Ar–H), 1653 (C=O), 1605 (C=N), 1286 (C–O–C) cm<sup>−1</sup>; <sup>1</sup>H NMR (400 MHz, DMSO-*d*<sub>6</sub>) δ ppm: 2.33 (s, 3H, CH<sub>3</sub>), 5.16 (s, 2H, OCH<sub>2</sub>), 5.40 (s, 2H, OH), 6.30 (t, 2H, *J* = 2.0, pyrrole–C<sub>3</sub>, C<sub>4</sub>–H), 6.82–6.91 (m, 2H, phenoxy–C<sub>2</sub>, C<sub>6</sub>–H), 7.17–7.22 (m, 2H, phenoxy–C<sub>3</sub>, C<sub>5</sub>–H), 7.26 (t, 2H, *J* = 2.0, pyrrole–C<sub>2</sub>, C<sub>5</sub>–H), 7.49 (d, 2H, *J* = 8.7, phenyl–C<sub>3</sub>, C<sub>5</sub>–H), 7.83 (d, 2H, *J* = 8.6, phenyl–C<sub>2</sub>, C<sub>6</sub>–H), 10.83 (s, 1H, NH); <sup>13</sup>C NMR (100 MHz, DMSO-*d*<sub>6</sub>) δ ppm: 13.31,

65.35, 110.79, 115.69, 116.87, 119.93, 129.39, 129.80, 133.22, 140.99, 145.39, 150.65, 150.77, 169.81; MS (ESI):  $m/z$  = found 349.21 [M $^+$ ]; calcd. 349.14. Anal. Calcd. for C<sub>20</sub>H<sub>19</sub>N<sub>3</sub>O<sub>3</sub>: C, 68.75; H, 5.48; N, 12.03. Found: C, 69.03; H, 5.46; N, 12.08.

#### 4.7.17. N'-(1-(4-(1H-Pyrrol-1-yl)phenyl)ethylidene)-2-(2,4,6-trichlorophenoxy)acetohydrazide (**4q**)

(Yield 63%). mp 256–258 °C; FTIR (KBr): 3212 (NH), 3109, 2923 (Ar–H), 1689 (C=O), 1606 (C=N), 1257 (C–O–C), 715 (C–Cl) cm $^{-1}$ ;  $^1$ H NMR (400 MHz, DMSO- $d_6$ )  $\delta$  ppm: 2.32 (s, 3H, CH<sub>3</sub>), 5.21 (s, 2H, OCH<sub>2</sub>), 6.31 (t, 2H,  $J$  = 2.1, pyrrole–C<sub>3</sub>, C<sub>4</sub>–H), 7.25 (t, 2H,  $J$  = 2.0, pyrrole–C<sub>2</sub>, C<sub>5</sub>–H), 7.45–7.49 (m, 2H, phenoxy–C<sub>3</sub>, C<sub>5</sub>–H), 7.51 (d, 2H,  $J$  = 8.6, phenyl–C<sub>3</sub>, C<sub>5</sub>–H), 7.81 (d, 2H,  $J$  = 8.6, phenyl–C<sub>2</sub>, C<sub>6</sub>–H), 10.87 (s, 1H, NH);  $^{13}$ C NMR (100 MHz, DMSO- $d_6$ )  $\delta$  ppm: 13.36, 65.80, 110.78, 120.00, 129.31, 129.43, 129.87, 129.91, 133.49, 141.88, 145.88, 152.33, 169.89; MS (ESI):  $m/z$  = found 435.27 [M $^+$ ], 437.22 [M $^+$ +2]; calcd. 435.03. Anal. Calcd. for C<sub>20</sub>H<sub>16</sub>Cl<sub>3</sub>N<sub>3</sub>O<sub>2</sub>: C, 55.00; H, 3.69; N, 9.62. Found: C, 54.78; H, 3.70; N, 9.66.

#### 4.7.18. N'-(1-(4-(1H-Pyrrol-1-yl)phenyl)ethylidene)-2-(naphthalen-1-yloxy)acetohydrazide (**4r**)

(Yield 71%). mp 210–212 °C; FTIR (KBr): 3191 (NH), 3093, 2922 (Ar–H), 1706 (C=O), 1612 (C=N), 1326 (C–O–C) cm $^{-1}$ ;  $^1$ H NMR (400 MHz, DMSO- $d_6$ )  $\delta$  ppm: 2.30 (s, 3H, CH<sub>3</sub>), 5.36 (s, 2H, OCH<sub>2</sub>), 6.26 (t, 2H,  $J$  = 2.1, pyrrole–C<sub>3</sub>, C<sub>4</sub>–H), 6.84 (d, 1H,  $J$  = 7.5, naphthoxy–C<sub>2</sub>–H), 7.28 (t, 2H,  $J$  = 2.0, pyrrole–C<sub>2</sub>, C<sub>5</sub>–H), 7.33–7.37 (m, 1H, naphthoxy–C<sub>3</sub>–H), 7.42–7.53 (m, 5H, phenyl–C<sub>3</sub>, C<sub>5</sub>–H and naphthoxy–C<sub>4</sub>, C<sub>6</sub>, C<sub>7</sub>–H), 7.80–7.88 (m, 3H, naphthoxy–C<sub>5</sub>–H and ph–C<sub>2</sub>, C<sub>6</sub>–H), 8.30 (t, 1H,  $J$  = 2.3, naphthoxy–C<sub>8</sub>–H), 10.88 (s, 1H, NH);  $^{13}$ C NMR (100 MHz, DMSO- $d_6$ )  $\delta$  ppm: 13.38, 65.53, 110.65, 118.62, 118.83, 120.04, 121.80, 124.97, 125.76, 126.22, 127.17, 127.34, 134.01, 134.68, 140.30, 147.54, 153.60, 169.48; MS (ESI):  $m/z$  = found 383.05 [M $^+$ ]; calcd. 383.16. Anal. Calcd. for C<sub>24</sub>H<sub>21</sub>N<sub>3</sub>O<sub>2</sub>: C, 75.18; H, 5.52; N, 10.96. Found: C, 74.88; H, 5.54; N, 10.92.

#### 4.7.19. N'-(1-(4-(1H-Pyrrol-1-yl)phenyl)ethylidene)-2-(naphthalen-2-yloxy)acetohydrazide (**4s**)

(Yield 68%). mp 208–210 °C; FTIR (KBr): 3363 (NH), 3138, 2924, 2857 (Ar–H), 1690 (C=O), 1607 (C=N), 1328 (C–O–C) cm $^{-1}$ ;  $^1$ H NMR (400 MHz, DMSO- $d_6$ )  $\delta$  ppm: 2.30 (s, 3H, CH<sub>3</sub>), 5.24 (s, 2H, OCH<sub>2</sub>), 6.25 (t, 2H,  $J$  = 2.0, pyrrole–C<sub>3</sub>, C<sub>4</sub>–H), 7.13 (s, 1H, naphthoxy–C<sub>3</sub>–H), 7.18 (t, 2H,  $J$  = 2.1, pyrrole–C<sub>2</sub>, C<sub>5</sub>–H), 7.21–7.29 (m, 2H, naphthoxy–C<sub>1</sub>, C<sub>6</sub>–H), 7.37 (s, 1H, naphthoxy–C<sub>7</sub>–H), 7.46 (d, 2H,  $J$  = 8.6, phenyl–C<sub>3</sub>, C<sub>5</sub>–H), 7.68–7.74 (m, 3H, naphthoxy–C<sub>4</sub>, C<sub>5</sub>, C<sub>8</sub>–H), 7.84 (d, 2H,  $J$  = 8.7, phenyl–C<sub>2</sub>, C<sub>6</sub>–H), 10.79 (s, 1H, NH);  $^{13}$ C NMR (100 MHz, DMSO- $d_6$ )  $\delta$  ppm: 13.40, 65.39, 105.90, 110.63, 118.56, 118.78, 124.01, 126.63, 126.79, 127.31, 129.33, 129.49, 129.79, 133.73, 141.78, 145.67, 155.63, 169.70; MS (ESI):  $m/z$  = found 384.17 [M $^+$ +1], 385.17 [M $^+$ +2]; calcd. 383.16. Anal. Calcd. for C<sub>24</sub>H<sub>21</sub>N<sub>3</sub>O<sub>2</sub>: C, 75.18; H, 5.52; N, 10.96. Found: C, 75.48; H, 5.50; N, 10.92.

#### 4.7.20. N'-(1-(4-(1H-Pyrrol-1-yl)phenyl)ethylidene)-4-methylbenzenesulfonohydrazide (**4t**)

(Yield 70%). mp 210–212 °C; FTIR (KBr): 3201 (NH), 3066, 3041, 2923 (Ar–H), 1606 (C=N), 1336 (SO<sub>2</sub><sup>asym</sup>), 1168 (SO<sub>2</sub><sup>sym</sup>) cm $^{-1}$ ;  $^1$ H NMR (400 MHz, DMSO- $d_6$ )  $\delta$  ppm: 2.21 (s, 3H, CH<sub>3</sub>), 2.42 (s, 3H, sulfonamidephenyl–CH<sub>3</sub>), 6.29 (s, 2H, pyrrole–C<sub>3</sub>, C<sub>4</sub>–H), 7.18 (s, 2H, pyrrole–C<sub>2</sub>, C<sub>5</sub>–H), 7.36 (d, 2H,  $J$  = 7.9, sulfonamidephenyl–C<sub>3</sub>, C<sub>5</sub>–H), 7.43 (d, 2H,  $J$  = 8.6, phenyl–C<sub>3</sub>, C<sub>5</sub>–H), 7.70 (d, 2H,  $J$  = 8.6, sulfonamidephenyl–C<sub>2</sub>, C<sub>6</sub>–H), 7.86 (d, 2H,  $J$  = 8.1, phenyl–C<sub>2</sub>, C<sub>6</sub>–H), 10.37 (s, 1H, NH);  $^{13}$ C NMR (100 MHz, DMSO- $d_6$ )  $\delta$  ppm: 14.05, 21.06, 110.67, 118.62, 118.72, 127.20, 127.53, 129.20, 134.09, 136.20, 140.40, 143.05, 152.09; MS (ESI):  $m/z$  = found 353.01 [M $^+$ ]; calcd. 353.12. Anal. Calcd. for C<sub>19</sub>H<sub>19</sub>N<sub>3</sub>O<sub>2</sub>S: C, 64.57; H, 5.42; N, 11.89. Found: C, 64.83; H, 5.40; N, 11.94.

#### 4.7.21. N-(4-((2-(1-(4-(1H-Pyrrol-1-yl)phenyl)ethylidene)hydrazinyl)sulfonyl)phenyl)acetamide (**4u**)

(Yield 70%). mp 256–258 °C (D); FTIR (KBr): 3369 (NH), 3111, 2924, 2855 (Ar–H), 1681 (C=O), 1594 (C=N), 1329 (SO<sub>2</sub><sup>asym</sup>), 1156 (SO<sub>2</sub><sup>sym</sup>) cm $^{-1}$ ;  $^1$ H NMR (400 MHz, DMSO- $d_6$ )  $\delta$  ppm: 2.13 (s, 3H, COCH<sub>3</sub>), 2.21 (s, 3H, CH<sub>3</sub>), 6.28 (s, 2H, pyrrole–C<sub>3</sub>, C<sub>4</sub>–H), 7.18 (s, 2H, pyrrole–C<sub>2</sub>, C<sub>5</sub>–H), 7.43 (d, 2H,  $J$  = 8.7, phenyl–C<sub>3</sub>, C<sub>5</sub>–H), 7.70 (d, 2H,  $J$  = 8.7, sulfonamidephenyl–C<sub>3</sub>, C<sub>5</sub>–H), 7.79 (d, 2H,  $J$  = 8.6, phenyl–C<sub>2</sub>, C<sub>6</sub>–H), 7.87 (d, 2H,  $J$  = 8.8, sulfonamidephenyl–C<sub>2</sub>, C<sub>6</sub>–H), 10.14 (s, 1H, CONH), 10.31 (s, 1H, NH);  $^{13}$ C NMR (100 MHz, DMSO- $d_6$ )  $\delta$  ppm: 13.97, 24.01, 110.62, 118.24, 118.53, 118.75, 127.14, 128.52, 132.51, 134.16, 140.40, 143.15, 151.87, 168.75; MS (ESI):  $m/z$  = found 395.11 [M $^+$ –1], 396.11 [M $^+$ ]; calcd. 396.13. Anal. Calcd. for C<sub>20</sub>H<sub>20</sub>N<sub>4</sub>O<sub>3</sub>S: C, 60.59; H, 5.08; N, 14.13. Found: C, 60.83; H, 5.06; N, 14.07.

#### 4.7.22. N'-(1-(4-(1H-Pyrrol-1-yl)phenyl)ethylidene)-4-aminobenzenesulfonohydrazide (**4v**)

(Yield 62%). mp 225–227 °C; FTIR (KBr): 3274, 3085 (NH), 2957 (Ar–H), 1513 (C=N), 1316 (SO<sub>2</sub><sup>asym</sup>), 1129 (SO<sub>2</sub><sup>sym</sup>) cm $^{-1}$ ;  $^1$ H NMR (400 MHz, DMSO- $d_6$ )  $\delta$  ppm: 2.20 (s, 3H, CH<sub>3</sub>), 6.29 (s, 2H, pyrrole–C<sub>3</sub>, C<sub>4</sub>–H), 6.37 (s, 1H, NH<sub>2</sub>), 7.18 (s, 2H, pyrrole–C<sub>2</sub>, C<sub>5</sub>–H), 7.02 (d, 2H,  $J$  = 7.9, sulfonamidephenyl–C<sub>3</sub>, C<sub>5</sub>–H), 7.47 (d, 2H,  $J$  = 8.2, phenyl–C<sub>3</sub>, C<sub>5</sub>–H), 7.71 (d, 2H,  $J$  = 8.3, sulfonamidephenyl–C<sub>2</sub>, C<sub>6</sub>–H), 7.84 (d, 2H,  $J$  = 8.3, phenyl–C<sub>2</sub>, C<sub>6</sub>–H), 10.35 (s, 1H, NH);  $^{13}$ C NMR (100 MHz, DMSO- $d_6$ )  $\delta$  ppm: 13.83, 110.73, 112.29, 119.20, 127.09, 128.49, 130.03, 134.08, 136.00, 142.60, 151.62, 168.22; MS (ESI):  $m/z$  = found 354.41 [M $^+$ ]; calcd. 354.12. Anal. Calcd. for C<sub>18</sub>H<sub>18</sub>N<sub>4</sub>O<sub>2</sub>S: C, 61.00; H, 5.12; N, 15.81. Found: C, 61.24; H, 5.10; N, 15.87.

#### 4.7.23. 1-(4-(1-(2-Phenylhydrazono)ethyl)phenyl)-1H-pyrrole (**4w**)

(Yield 69%). mp 195–197 °C; FTIR (KBr): 3350 (NH), 3138, 2923, 2856 (Ar–H), 1600 (C=N) cm $^{-1}$ ;  $^1$ H NMR (400 MHz, DMSO- $d_6$ )  $\delta$  ppm: 2.28 (s, 3H, CH<sub>3</sub>), 6.27 (t, 2H,  $J$  = 2.1, pyrrole–C<sub>3</sub>, C<sub>4</sub>–H), 6.77 (m, 1H, hydrazonophenyl–C<sub>4</sub>–H), 7.17–7.24 (m, 4H, hydrazonophenyl–C<sub>2</sub>, C<sub>3</sub>, C<sub>5</sub>, C<sub>6</sub>–H), 7.26 (t, 2H,  $J$  = 2.1, pyrrole–C<sub>2</sub>, C<sub>5</sub>–H), 7.50 (dd, 2H,  $J$  = 2.0, 1.9, phenyl–C<sub>3</sub>, C<sub>5</sub>–H), 7.84–7.87 (m, 2H, phenyl–C<sub>2</sub>, C<sub>6</sub>–H), 9.15 (s, 1H, NH);  $^{13}$ C NMR (100 MHz, DMSO- $d_6$ )  $\delta$  ppm: 17.00, 110.56, 112.99, 119.24, 126.17, 128.80, 129.77, 135.09, 142.80, 143.11, 169.77; MS (ESI):  $m/z$  = found 275.37 [M $^+$ ]; calcd. 275.14. Anal. Calcd. for C<sub>18</sub>H<sub>17</sub>N<sub>3</sub>: C, 78.52; H, 6.22; N, 15.26. Found: C, 78.21; H, 6.25; N, 15.32.

#### 4.7.24. 1-(4-(1-(2-(2,4-Dinitrophenyl)hydrazono)ethyl)phenyl)-1H-pyrrole (**4x**)

(Yield 70%). mp 246–248 °C; FTIR (KBr): 3306 (NH), 3102, 2922, 2854 (Ar–H), 1614 (C=N), 1509 (NO<sub>2</sub><sup>asym</sup>), 1259 (NO<sub>2</sub><sup>sym</sup>) cm $^{-1}$ ;  $^1$ H NMR (400 MHz, DMSO- $d_6$ )  $\delta$  ppm: 2.51 (s, 3H, CH<sub>3</sub>), 6.32 (t, 2H,  $J$  = 2.0, pyrrole–C<sub>3</sub>, C<sub>4</sub>–H), 7.30 (t, 2H,  $J$  = 2.0, pyrrole–C<sub>2</sub>, C<sub>5</sub>–H), 7.59 (d, 2H,  $J$  = 8.7, phenyl–C<sub>3</sub>, C<sub>5</sub>–H), 8.02 (d, 2H,  $J$  = 8.7, phenyl–C<sub>2</sub>, C<sub>6</sub>–H), 8.17 (d, 1H,  $J$  = 9.6, dinitrophenyl–C<sub>6</sub>–H), 8.43 (dd, 1H,  $J$  = 2.6, 2.5, dinitrophenyl–C<sub>5</sub>–H), 9.03 (d, 1H,  $J$  = 2.6, dinitrophenyl–C<sub>3</sub>–H), 11.29 (s, 1H, NH);  $^{13}$ C NMR (100 MHz, DMSO- $d_6$ )  $\delta$  ppm: 17.00, 110.83, 116.12, 118.64, 122.73, 127.88, 128.03, 135.26, 139.01, 143.35, 145.20, 168.80; MS (ESI):  $m/z$  = found 365.01 [M $^+$ ]; calcd. 365.11. Anal. Calcd. for C<sub>18</sub>H<sub>15</sub>N<sub>5</sub>O<sub>4</sub>: C, 59.18; H, 4.14; N, 19.17. Found: C, 58.94; H, 4.16; N, 19.09.

#### 4.7.25. 2-(1-(4-(1H-Pyrrol-1-yl)phenyl)ethylidene)hydrazinecarbothioamide (**4y**)

(Yield 79%). mp 256–258 °C; FTIR (KBr): 3414, 3263 (NH), 2924, 2856 (Ar–H), 1605 (C=N) cm $^{-1}$ ;  $^1$ H NMR (400 MHz, DMSO- $d_6$ )  $\delta$  ppm: 2.30 (s, 3H, CH<sub>3</sub>), 6.24 (s, 2H, pyrrole–C<sub>3</sub>, C<sub>4</sub>–H), 7.16 (s, 2H, pyrrole–C<sub>2</sub>, C<sub>5</sub>–H), 7.42 (d, 2H,  $J$  = 8.5, phenyl–C<sub>3</sub>, C<sub>5</sub>–H), 7.87 (d,

2H,  $J = 8.5$ , phenyl—C<sub>2</sub>, C<sub>6</sub>—H), 8.05 (s, 2H, NH<sub>2</sub>), 10.00 (s, 1H, NH); <sup>13</sup>C NMR (100 MHz, DMSO-d<sub>6</sub>) δ ppm: 13.77, 110.61, 118.61, 118.68, 127.75, 134.40, 140.33, 146.74, 178.84; MS (ESI):  $m/z$  = found 258.03 [M<sup>+</sup>]; calcd. 258.09. Anal. Calcd. for C<sub>13</sub>H<sub>14</sub>N<sub>4</sub>S: C, 60.44; H, 5.46; N, 21.69. Found: C, 60.68; H, 5.44; N, 21.60.

#### 4.7.26. 2-(1-(4-(1H-Pyrrol-1-yl)phenyl)ethylidene)hydrazinecarboxamide (**4z**)

(Yield 77%). mp 277–279 °C; FTIR (KBr): 3478, 3273 (NH), 3138, 2925 (Ar—H), 1749 (C=O), 1583 (C=N) cm<sup>-1</sup>; <sup>1</sup>H NMR (400 MHz, DMSO-d<sub>6</sub>) δ ppm: 2.20 (s, 3H, CH<sub>3</sub>), 6.25 (t, 2H,  $J = 2.1$ , pyrrole—C<sub>3</sub>, C<sub>4</sub>—H), 6.37 (s, 2H, NH<sub>2</sub>), 7.26 (t, 2H,  $J = 2.1$ , pyrrole—C<sub>2</sub>, C<sub>5</sub>—H), 7.48 (m, 2H, phenyl—C<sub>3</sub>, C<sub>5</sub>—H), 7.86 (m, 2H, phenyl—C<sub>3</sub>, C<sub>4</sub>—H), 9.27 (s, 1H, NH); <sup>13</sup>C NMR (100 MHz, DMSO-d<sub>6</sub>) δ ppm: 13.12, 110.46, 118.52, 118.81, 126.98, 135.15, 139.80, 143.26, 157.26; MS (ESI):  $m/z$  = found 242.17 [M<sup>+</sup>]; calcd. 242.12. Anal. Calcd. for C<sub>13</sub>H<sub>14</sub>N<sub>4</sub>O: C, 64.45; H, 5.82; N, 23.13. Found: C, 64.71; H, 5.80; N, 23.22.

#### 4.7.27. N'-(1-(4-(2,5-Dimethyl-1H-pyrrol-1-yl)phenyl)ethylidene)isonicotinohydrazide (**5a**)

(Yield 69%). mp 216–216 °C; FTIR (KBr): 3185 (NH), 3072, 2977 (Ar—H), 1660 (C=O), 1549 (C=N) cm<sup>-1</sup>; <sup>1</sup>H NMR (400 MHz, DMSO-d<sub>6</sub>) δ ppm: 2.01 (s, 6H, 2CH<sub>3</sub>), 2.45 (s, 3H, CH<sub>3</sub>), 5.80 (s, 2H, pyrrole—C<sub>3</sub>, C<sub>4</sub>—H), 7.29 (d, 2H,  $J = 8.3$ , phenyl—C<sub>3</sub>, C<sub>5</sub>—H), 7.83 (d, 2H,  $J = 5.4$ , pyridine—C<sub>2</sub>, C<sub>6</sub>—H), 7.99 (d, 2H,  $J = 8.3$ , phenyl—C<sub>2</sub>, C<sub>6</sub>—H), 8.76 (d, 2H,  $J = 5.1$ , pyridine—C<sub>3</sub>, C<sub>5</sub>—H), 11.10 (s, 1H, NH); <sup>13</sup>C NMR (75 MHz, DMSO-d<sub>6</sub>) δ ppm: 13.34, 15.23, 106.70, 122.37, 128.00, 128.35, 137.58, 140.03, 141.66, 150.59, 156.64, 162.96; MS (ESI):  $m/z$  = found 333.17 [M<sup>+</sup> + 1], 334.17 [M<sup>+</sup> + 2]; calcd. 332.16. Anal. Calcd. for C<sub>20</sub>H<sub>20</sub>N<sub>4</sub>O: C, 72.27; H, 6.06; N, 16.86. Found: C, 71.98; H, 6.08; N, 16.79.

#### 4.7.28. N'-(1-(4-(2,5-Dimethyl-1H-pyrrol-1-yl)phenyl)ethylidene)nicotinohydrazide (**5b**)

(Yield 72%). mp 184–186 °C; FTIR (KBr): 3247 (NH), 3051, 2978, 2919 (Ar—H), 1670 (C=O), 1588 (C=N) cm<sup>-1</sup>; <sup>1</sup>H NMR (400 MHz, DMSO-d<sub>6</sub>) δ ppm: 2.01 (s, 6H, 2CH<sub>3</sub>), 2.46 (s, 3H, CH<sub>3</sub>), 5.82 (s, 2H, pyrrole—C<sub>3</sub>, C<sub>4</sub>—H), 7.27 (d, 2H,  $J = 7.4$ , phenyl—C<sub>3</sub>, C<sub>5</sub>—H), 7.51 (dd, 1H,  $J = 5.0$ , pyridine—C<sub>5</sub>—H), 7.99 (d, 2H,  $J = 7.1$ , phenyl—C<sub>2</sub>, C<sub>6</sub>—H), 8.25–9.09 (m, 3H, pyridine—C<sub>2</sub>, C<sub>4</sub>, C<sub>6</sub>—H), 11.04 (s, 1H, NH); <sup>13</sup>C NMR (100 MHz, DMSO-d<sub>6</sub>) δ ppm: 12.81, 14.69, 106.03, 123.15, 126.64, 127.23, 127.47, 127.68, 129.61, 135.64, 137.12, 139.33, 148.78, 151.82, 162.58; MS (ESI):  $m/z$  = found 333.17 [M<sup>+</sup> + 1], 334.17 [M<sup>+</sup> + 2]; calcd. 332.16. Anal. Calcd. for C<sub>20</sub>H<sub>20</sub>N<sub>4</sub>O: C, 72.27; H, 6.06; N, 16.86. Found: C, 72.56; H, 6.04; N, 16.79.

#### 4.7.29. N'-(1-(4-(2,5-Dimethyl-1H-pyrrol-1-yl)phenyl)ethylidene)-4-(1H-pyrrol-1-yl)benzohydrazide (**5c**)

(Yield 65%). mp 271–219 °C; FTIR (KBr): 3270 (NH), 3074, 2977, 2920 (Ar—H), 1666 (C=O), 1608 (C=N) cm<sup>-1</sup>; <sup>1</sup>H NMR (400 MHz, DMSO-d<sub>6</sub>) δ ppm: 2.00 (s, 6H, 2CH<sub>3</sub>), 2.44 (s, 3H, CH<sub>3</sub>), 5.80 (s, 2H, pyrrole—C<sub>3</sub>, C<sub>4</sub>—H), 6.31 (t, 2H,  $J = 2.1$ , pyrrole—C<sub>3</sub>, C<sub>4</sub>—H), 7.30 (d, 2H,  $J = 7.2$ , phenyl—C<sub>3</sub>, C<sub>5</sub>—H), 7.44 (t, 2H,  $J = 2.0$ , pyrrole—C<sub>2</sub>, C<sub>5</sub>—H), 7.71 (d, 2H,  $J = 8.3$ , hydrazide—phenyl—C<sub>3</sub>, C<sub>5</sub>—H), 8.00 (s, 4H, phenyl—C<sub>2</sub>, C<sub>6</sub>—H & hydrazide—phenyl—C<sub>2</sub>, C<sub>6</sub>—H), 10.87 (s, 1H, NH); <sup>13</sup>C NMR (100 MHz, DMSO-d<sub>6</sub>) δ ppm: 12.84, 16.11, 106.04, 111.02, 118.83, 127.46, 128.83, 129.13, 130.09, 135.11, 142.11, 144.27, 149.21, 164.20; MS (ESI):  $m/z$  = found 396.36 [M<sup>+</sup>]; calcd. 396.20. Anal. Calcd. for C<sub>25</sub>H<sub>24</sub>N<sub>4</sub>O: C, 75.73; H, 6.10; N, 14.13. Found: C, 76.03; H, 6.08; N, 14.19.

#### 4.7.30. 4-(2,5-Dimethyl-1H-pyrrol-1-yl)-N'-(1-(4-(2,5-dimethyl-1H-pyrrol-1-yl)phenyl)ethylidene)benzohydrazide (**5d**)

(Yield 66%). mp 186–188 °C; FTIR (KBr): 3200 (NH), 2971, 2921 (Ar—H), 1652 (C=O), 1609 (C=N) cm<sup>-1</sup>; <sup>1</sup>H NMR (400 MHz, DMSO-

d<sub>6</sub>) δ ppm: 2.01 (s, 6H, 2CH<sub>3</sub>), 2.03 (s, 6H, 2CH<sub>3</sub>), 2.46 (s, 3H, CH<sub>3</sub>), 5.83 (d, 4H, pyrrole—C<sub>3</sub>, C<sub>4</sub>—H and hydrazide—pyrrole—C<sub>3</sub>, C<sub>4</sub>—H), 7.27–8.06 (m, 8H, phenyl—C<sub>2</sub>, C<sub>3</sub>, C<sub>5</sub>, C<sub>6</sub>—H and hydrazide—phenyl—C<sub>2</sub>, C<sub>3</sub>, C<sub>5</sub>, C<sub>6</sub>—H), 10.96 (s, 1H, NH); <sup>13</sup>C NMR (100 MHz, DMSO-d<sub>6</sub>) δ ppm: 12.80, 12.86, 15.20, 106.01, 106.30, 127.47, 127.64, 128.20, 128.71, 129.09, 129.25, 135.17, 139.77, 143.09, 148.22, 163.20; MS (ESI):  $m/z$  = found 425.23 [M<sup>+</sup> + 1], 426.23 [M<sup>+</sup> + 2]; calcd. 424.23. Anal. Calcd. for C<sub>27</sub>H<sub>28</sub>N<sub>4</sub>O: C, 76.39; H, 6.65; N, 13.20. Found: C, 76.08; H, 6.68; N, 13.25.

#### 4.7.31. N'-(1-(4-(2,5-Dimethyl-1H-pyrrol-1-yl)phenyl)ethylidene)benzohydrazide (**5e**)

(Yield 69%). mp 190–192 °C; FTIR (KBr): 3254 (NH), 3038, 2923, 2856 (Ar—H), 1668 (C=O), 1606 (C=N) cm<sup>-1</sup>; <sup>1</sup>H NMR (400 MHz, DMSO-d<sub>6</sub>) δ ppm: 2.00 (s, 6H, 2CH<sub>3</sub>), 2.40 (s, 3H, CH<sub>3</sub>), 5.81 (s, 2H, pyrrole—C<sub>3</sub>, C<sub>4</sub>—H), 7.29–7.35 (m, 4H, hydrazide—phenyl—C<sub>3</sub>, C<sub>5</sub>—H and phenyl—C<sub>3</sub>, C<sub>5</sub>—H), 7.77–7.92 (m, 5H, phenyl—C<sub>2</sub>, C<sub>6</sub>—H and hydrazide—phenyl—C<sub>2</sub>, C<sub>3</sub>, C<sub>6</sub>—H), 10.69 (s, 1H, NH); <sup>13</sup>C NMR (100 MHz, DMSO-d<sub>6</sub>) δ ppm: 12.72, 13.41, 105.97, 127.43, 128.09, 128.72, 129.41, 129.80, 132.09, 132.66, 133.69, 140.62, 145.94, 161.39; MS (ESI):  $m/z$  = found 331.41 [M<sup>+</sup>]; calcd. 331.17. Anal. Calcd. for C<sub>21</sub>H<sub>21</sub>N<sub>3</sub>O: C, 76.11; H, 6.39; N, 12.68. Found: C, 75.81; H, 6.42; N, 12.63.

#### 4.7.32. N'-(1-(4-(2,5-Dimethyl-1H-pyrrol-1-yl)phenyl)ethylidene)-4-methylbenzohydrazide (**5f**)

(Yield 66%). mp 191–193 °C; FTIR (KBr): 3244 (NH), 3034, 2922, 2856 (Ar—H), 1665 (C=O), 1610 (C=N) cm<sup>-1</sup>; <sup>1</sup>H NMR (400 MHz, DMSO-d<sub>6</sub>) δ ppm: 2.01 (s, 6H, 2CH<sub>3</sub>), 2.42 (s, 3H, CH<sub>3</sub>), 2.54 (s, 3H, phenyl—CH<sub>3</sub>), 5.80 (s, 2H, pyrrole—C<sub>3</sub>, C<sub>4</sub>—H), 7.25 (d, 2H,  $J = 7.9$ , hydrazide—phenyl—C<sub>3</sub>, C<sub>5</sub>—H), 7.30 (d, 2H,  $J = 7.8$ , phenyl—C<sub>3</sub>, C<sub>5</sub>—H), 7.83 (s, 2H, phenyl—C<sub>2</sub>, C<sub>6</sub>—H), 7.95 (s, 2H, hydrazide—phenyl—C<sub>2</sub>, C<sub>6</sub>—H), 10.70 (s, 1H, NH); <sup>13</sup>C NMR (100 MHz, DMSO-d<sub>6</sub>) δ ppm: 12.79, 21.22, 106.20, 127.47, 127.63, 129.09, 129.52, 130.22, 135.29, 140.53, 142.31, 148.20, 164.00; MS (ESI):  $m/z$  = found 346.19 [M<sup>+</sup> + 1], 347.19 [M<sup>+</sup> + 2]; calcd. 345.18. Anal. Calcd. for C<sub>22</sub>H<sub>23</sub>N<sub>3</sub>O: C, 76.49; H, 6.71; N, 12.16. Found: C, 76.80; H, 6.68; N, 12.11.

#### 4.7.33. 4-Chloro-N'-(1-(4-(2,5-dimethyl-1H-pyrrol-1-yl)phenyl)ethylidene)benzohydrazide (**5g**)

(Yield 70%). mp 203–205 °C; FTIR (KBr): 3269 (NH), 3052, 2924 (Ar—H), 1654 (C=O), 1605 (C=N), 721 (C—Cl) cm<sup>-1</sup>; <sup>1</sup>H NMR (400 MHz, DMSO-d<sub>6</sub>) δ ppm: 1.99 (s, 6H, 2CH<sub>3</sub>), 2.30 (s, 3H, CH<sub>3</sub>), 5.81 (s, 2H, pyrrole—C<sub>3</sub>, C<sub>4</sub>—H), 7.40–7.63 (m, 4H, phenyl—C<sub>3</sub>, C<sub>5</sub>—H and 4-chlorophenyl—C<sub>3</sub>, C<sub>5</sub>—H), 7.79–7.90 (m, 4H, phenyl—C<sub>2</sub>, C<sub>6</sub>—H and 4-chlorophenyl—C<sub>3</sub>, C<sub>5</sub>—H), 10.80 (s, 1H, NH); <sup>13</sup>C NMR (100 MHz, DMSO-d<sub>6</sub>) δ ppm: 12.39, 13.37, 106.20, 127.09, 127.50, 128.33, 128.65, 129.05, 130.13, 133.50, 134.89, 140.09, 145.11, 161.05; MS (ESI):  $m/z$  = found 365.25 [M<sup>+</sup>], 367.21 [M<sup>+</sup>+2]; calcd. 365.13. Anal. Calcd. for C<sub>21</sub>H<sub>20</sub>ClN<sub>3</sub>O: C, 68.94; H, 5.51; N, 11.49. Found: C, 69.22; H, 5.49; N, 11.44.

#### 4.7.34. 4-Bromo-N'-(1-(4-(2,5-dimethyl-1H-pyrrol-1-yl)phenyl)ethylidene)benzohydrazide (**5h**)

(Yield 68%). mp 207–209 °C; FTIR (KBr): 3189 (NH), 3044, 2924, 2853 (Ar—H), 1650 (C=O), 1605 (C=N), 726 (C—Br) cm<sup>-1</sup>; <sup>1</sup>H NMR (400 MHz, DMSO-d<sub>6</sub>) δ ppm: 2.03 (s, 6H, 2CH<sub>3</sub>), 2.33 (s, 3H, CH<sub>3</sub>), 5.80 (s, 2H, pyrrole—C<sub>3</sub>, C<sub>4</sub>—H), 7.43–7.66 (m, 4H, phenyl—C<sub>3</sub>, C<sub>5</sub>—H and 4-bromophenyl—C<sub>3</sub>, C<sub>5</sub>—H), 7.80–7.93 (m, 4H, phenyl—C<sub>2</sub>, C<sub>6</sub>—H and 4-bromophenyl—C<sub>3</sub>, C<sub>5</sub>—H), 10.87 (s, 1H, NH); <sup>13</sup>C NMR (100 MHz, DMSO-d<sub>6</sub>) δ ppm: 12.60, 14.21, 106.03, 127.10, 126.63, 127.49, 128.51, 129.23, 130.88, 131.09, 133.89, 141.00, 144.89, 162.09; MS (ESI):  $m/z$  = found 409.13 [M<sup>+</sup>], 411.07 [M<sup>+</sup>+2]; calcd. 409.08. Anal. Calcd. FOR C<sub>21</sub>H<sub>20</sub>BrN<sub>3</sub>O: C, 61.47; H, 4.91; N, 10.24. Found: C, 61.72; H, 4.89; N, 10.20.

**4.7.35. 2-Chloro-N'-(1-(4-(2,5-dimethyl-1H-pyrrol-1-yl)phenyl)ethylidene)benzohydrazide (**5i**)**

(Yield 65%). mp 200–202 °C; FTIR (KBr): 3246 (NH), 3019, 2923 (Ar–H), 1665 (C=O), 1617 (C=N), 761 (C–Cl) cm<sup>-1</sup>; <sup>1</sup>H NMR (400 MHz, DMSO-*d*<sub>6</sub>) δ ppm: 2.01 (s, 6H, 2CH<sub>3</sub>), 2.33 (s, 3H, CH<sub>3</sub>), 5.83 (s, 2H, pyrrole–C<sub>3</sub>, C<sub>4</sub>–H), 7.41–7.53 (m, 4H, 2-chlorophenyl–C<sub>5</sub>, C<sub>6</sub>–H and phenyl–C<sub>3</sub>, C<sub>5</sub>–H), 7.67–7.72 (m, 2H, 2-chlorophenyl–C<sub>3</sub>, C<sub>4</sub>–H), 7.83–7.89 (m, 2H, ph–C<sub>2</sub>, C<sub>6</sub>–H), 10.87 (s, 1H, NH); <sup>13</sup>C NMR (100 MHz, DMSO-*d*<sub>6</sub>) δ ppm: 12.59, 14.22, 106.01, 127.33, 126.87, 128.56, 129.29, 129.81, 130.10, 131.78, 133.09, 134.27, 134.57, 142.05, 145.31, 162.23; MS (ESI): *m/z* = found 365.01 [M<sup>+</sup>], 367.34 [M<sup>+</sup> + 2]; calcd. 365.13. Anal. Calcd. for C<sub>21</sub>H<sub>20</sub>ClN<sub>3</sub>O<sub>2</sub>: C, 68.94; H, 5.51; N, 11.49. Found: C, 69.22; H, 5.49; N, 11.54.

**4.7.36. N'-(1-(4-(2,5-Dimethyl-1H-pyrrol-1-yl)phenyl)ethylidene)-4-hydroxybenzohydrazide (**5j**)**

(Yield 63%). mp 277–278 °C; FTIR (KBr): 3442 (OH), 3241 (NH), 3017, 2924 (Ar–H), 1663 (C=O), 1607 (C=N) cm<sup>-1</sup>; <sup>1</sup>H NMR (400 MHz, DMSO-*d*<sub>6</sub>) δ ppm: 2.00 (s, 6H, 2CH<sub>3</sub>), 2.33 (s, 3H, CH<sub>3</sub>), 5.31 (s, 1H, OH), 5.81 (s, 2H, pyrrole–C<sub>3</sub>, C<sub>4</sub>–H), 6.81–6.92 (m, 2H, 4-hydroxyphenyl–C<sub>3</sub>, C<sub>5</sub>–H), 7.48 (d, 2H, *J* = 8.6, phenyl–C<sub>3</sub>, C<sub>5</sub>–H), 7.70–7.89 (m, 4H phenyl–C<sub>2</sub>, C<sub>6</sub>–H and 4-hydroxyphenyl–C<sub>2</sub>, C<sub>6</sub>–H), 10.88 (s, 1H, NH); <sup>13</sup>C NMR (100 MHz, DMSO-*d*<sub>6</sub>) δ ppm: 12.27, 14.29, 106.01, 116.03, 125.40, 127.89, 128.88, 129.35, 129.83, 132.60, 141.01, 145.37, 161.90, 162.78; MS (ESI): *m/z* = found 347.56 [M<sup>+</sup>]; calcd. 347.16. Anal. Calcd. for C<sub>21</sub>H<sub>21</sub>N<sub>3</sub>O<sub>2</sub>: C, 72.60; H, 6.09; N, 12.10. Found: C, 72.31; H, 6.11; N, 12.15.

**4.7.37. N'-(1-(4-(2,5-Dimethyl-1H-pyrrol-1-yl)phenyl)ethylidene)-2-phenoxyacetohydrazide (**5k**)**

(Yield 70%). mp 197–199 °C; FTIR (KBr): 3365 (NH), 3062, 2922 (Ar–H), 1706 (C=O), 1602 (C=N), 1293 (C–O–C) cm<sup>-1</sup>; <sup>1</sup>H NMR (400 MHz, DMSO-*d*<sub>6</sub>) δ ppm: 1.99 (s, 6H, 2CH<sub>3</sub>), 2.31 (s, 3H, CH<sub>3</sub>), 5.15 (s, 2H, OCH<sub>2</sub>), 5.81 (s, 2H, pyrrole–C<sub>3</sub>, C<sub>4</sub>–H), 6.89–7.03 (m, 3H, phenoxy–C<sub>2</sub>, C<sub>4</sub>, C<sub>6</sub>–H), 7.33–7.48 (m, 4H, phenoxy–C<sub>3</sub>, C<sub>5</sub>–H and phenyl–C<sub>3</sub>, C<sub>5</sub>–H), 7.90 (m, 2H, phenyl–C<sub>2</sub>, C<sub>6</sub>–H), 10.83 (s, 1H, NH); <sup>13</sup>C NMR (100 MHz, DMSO-*d*<sub>6</sub>) δ ppm: 12.29, 13.40, 65.40, 105.99, 114.30, 121.00, 128.01, 129.33, 129.78, 129.85, 133.89, 140.88, 146.01, 157.35, 170.01; MS (ESI): *m/z* = found 361.02 [M<sup>+</sup>]; calcd. 361.18. Anal. Calcd. for C<sub>22</sub>H<sub>23</sub>N<sub>3</sub>O<sub>2</sub>: C, 73.11; H, 6.41; N, 11.63. Found: C, 72.82; H, 6.44; N, 11.58.

**4.7.38. N'-(1-(4-(2,5-Dimethyl-1H-pyrrol-1-yl)phenyl)ethylidene)-2-(*p*-tolyloxy)acetohydrazide (**5l**)**

(Yield 73%). mp 198–200 °C; FTIR (KBr): 3186 (NH), 3016, 2922 (Ar–H), 1690 (C=O), 1610 (C=N), 1235 (C–O–C) cm<sup>-1</sup>; <sup>1</sup>H NMR (400 MHz, DMSO-*d*<sub>6</sub>) δ ppm: 2.01 (s, 6H, 2CH<sub>3</sub>), 2.30 (s, 3H, CH<sub>3</sub>), 2.35 (s, 3H, phenoxy–CH<sub>3</sub>), 5.17 (s, 2H, OCH<sub>2</sub>), 5.83 (s, 2H, pyrrole–C<sub>3</sub>, C<sub>4</sub>–H), 6.88–7.13 (m, 4H, phenoxy–C<sub>2</sub>, C<sub>3</sub>, C<sub>5</sub>, C<sub>6</sub>–H), 7.50 (m, 2H, phenyl–C<sub>3</sub>, C<sub>5</sub>–H), 7.89 (m, 2H, phenyl–C<sub>2</sub>, C<sub>6</sub>–H), 10.85 (s, 1H, NH); <sup>13</sup>C NMR (100 MHz, DMSO-*d*<sub>6</sub>) δ ppm: 12.31, 13.37, 21.18, 65.39, 105.98, 114.20, 127.88, 129.30, 129.75, 130.00, 130.68, 133.93, 142.03, 145.89, 156.33, 169.89; MS (ESI): *m/z* = found 375.01 [M<sup>+</sup>]; calcd. 375.19. Anal. Calcd. for C<sub>25</sub>H<sub>29</sub>N<sub>3</sub>O<sub>2</sub>: C, 73.57; H, 6.71; N, 11.19. Found: C, 73.86; H, 6.68; N, 11.23.

**4.7.39. 2-(4-Chlorophenoxy)-N'-(1-(4-(2,5-dimethyl-1H-pyrrol-1-yl)phenyl)ethylidene)acetohydrazide (**5m**)**

(Yield 72%). mp 173–175 °C; FTIR (KBr): 3363 (NH), 3063, 2922 (Ar–H), 1698 (C=O), 1600 (C=N), 1243 (C–O–C), 750 (C–Cl) cm<sup>-1</sup>;

<sup>1</sup>H NMR (400 MHz, DMSO-*d*<sub>6</sub>) δ ppm: 1.99 (s, 6H, 2CH<sub>3</sub>), 2.31 (s, 3H, CH<sub>3</sub>), 5.22 (s, 2H, OCH<sub>2</sub>), 5.83 (s, 2H, pyrrole–C<sub>3</sub>, C<sub>4</sub>–H), 6.91–7.83 (m, 8H, phenoxy–C<sub>2</sub>, C<sub>3</sub>, C<sub>5</sub>, C<sub>6</sub>–H & phenyl–C<sub>2</sub>, C<sub>3</sub>, C<sub>5</sub>, C<sub>6</sub>–H), 10.97 (s, 1H, NH); <sup>13</sup>C NMR (100 MHz, DMSO-*d*<sub>6</sub>) δ ppm: 12.65, 13.40, 65.69, 105.97, 117.39, 126.53, 128.09, 129.35, 129.67, 130.72, 133.81, 140.37, 145.77, 156.09, 169.52; MS (ESI): *m/z* = found 395.26 [M<sup>+</sup>], 397.05 [M<sup>+</sup> + 2]; calcd. 395.14. Anal. Calcd. for C<sub>22</sub>H<sub>22</sub>ClN<sub>3</sub>O<sub>2</sub>: C, 66.75; H, 5.60; N, 10.61. Found: C, 66.48; H, 5.62; N, 10.65.

**4.7.40. 2-(4-Bromophenoxy)-N'-(1-(4-(2,5-dimethyl-1H-pyrrol-1-yl)phenyl)ethylidene)acetohydrazide (**5n**)**

(Yield 60%). mp 181–183 °C; FTIR (KBr): 3114 (NH), 2920 (Ar–H), 17004 (C=O), 1619 (C=N), 1281.00 (C–O–C), 712 (C–Br) cm<sup>-1</sup>; <sup>1</sup>H NMR (400 MHz, DMSO-*d*<sub>6</sub>) δ ppm: 2.00 (s, 6H, 2CH<sub>3</sub>), 2.33 (s, 3H, CH<sub>3</sub>), 5.19 (s, 2H, OCH<sub>2</sub>), 5.79 (s, 2H, pyrrole–C<sub>3</sub>, C<sub>4</sub>–H), 6.86–6.95 (m, 2H, phenoxy–C<sub>2</sub>, C<sub>6</sub>–H), 7.23–7.26 (m, 2H, phenoxy–C<sub>3</sub>, C<sub>5</sub>–H), 7.37–7.43 (m, 2H, phenyl–C<sub>3</sub>, C<sub>5</sub>–H), 7.91 (d, 2H, *J* = 8.4, phenyl–C<sub>2</sub>, C<sub>6</sub>–H), 10.96 (s, 1H, NH); <sup>13</sup>C NMR (100 MHz, DMSO-*d*<sub>6</sub>) δ ppm: 12.77, 13.42, 65.40, 105.94, 112.18, 116.49, 126.72, 127.50, 127.64, 131.74, 136.96, 138.96, 147.47, 157.40, 169.51; MS (ESI): *m/z* = found 439.51 [M<sup>+</sup>], 441.22 [M<sup>+</sup> + 2]; calcd. 439.09. Anal. Calcd. for C<sub>22</sub>H<sub>22</sub>BrN<sub>3</sub>O<sub>2</sub>: C, 60.01; H, 5.04; N, 9.54. Found: C, 59.77; H, 5.06; N, 9.50.

**4.7.41. 2-(2-Chlorophenoxy)-N'-(1-(4-(2,5-dimethyl-1H-pyrrol-1-yl)phenyl)ethylidene)acetohydrazide (**5o**)**

(Yield 67%). mp 163–165 °C; FTIR (KBr): 3169 (NH), 3017, 2922 (Ar–H), 1690 (C=O), 1613 (C=N), 1232 (C–O–C), 753 (C–Cl) cm<sup>-1</sup>; <sup>1</sup>H NMR (400 MHz, DMSO-*d*<sub>6</sub>) δ ppm: 1.99 (s, 6H, 2CH<sub>3</sub>), 2.33 (s, 3H, CH<sub>3</sub>), 5.32 (s, 2H, OCH<sub>2</sub>), 5.80 (s, 2H, pyrrole–C<sub>3</sub>, C<sub>4</sub>–H), 6.92–7.45 (m, 6H, phenoxy–C<sub>3</sub>, C<sub>4</sub>, C<sub>5</sub>, C<sub>6</sub>–H and phenyl–C<sub>3</sub>, C<sub>5</sub>–H), 7.94 (d, 2H, *J* = 8.4, phenyl–C<sub>2</sub>, C<sub>6</sub>–H), 10.99 (s, 1H, NH); <sup>13</sup>C NMR (100 MHz, DMSO-*d*<sub>6</sub>) δ ppm: 12.63, 13.38, 65.63, 105.99, 112.69, 122.39, 122.60, 127.73, 128.07, 129.33, 129.64, 132.19, 133.49, 140.22, 145.93, 154.34, 169.50; MS (ESI): *m/z* = found 395.18 [M<sup>+</sup>], 397.37 [M<sup>+</sup> + 2]; calcd. 395.14. Anal. Calcd. for C<sub>22</sub>H<sub>22</sub>ClN<sub>3</sub>O<sub>2</sub>: C, 66.75; H, 5.60; N, 10.61. Found: C, 67.02; H, 5.58; N, 10.57.

**4.7.42. N'-(1-(4-(2,5-Dimethyl-1H-pyrrol-1-yl)phenyl)ethylidene)-2-(4-hydroxyphenoxy)acetohydrazide (**5p**)**

(Yield 60%). mp 278–280 °C; FTIR (KBr): 3449 (OH), 3189 (NH), 3015, 2924 (Ar–H), 1688 (C=O), 1609 (C=N), 1242 (C–O–C) cm<sup>-1</sup>; <sup>1</sup>H NMR (400 MHz, DMSO-*d*<sub>6</sub>) δ ppm: 2.01 (s, 6H, 2CH<sub>3</sub>), 2.32 (s, 3H, CH<sub>3</sub>), 5.18 (s, 2H, OCH<sub>2</sub>), 5.37 (s, 2H, OH), 5.83 (s, 2H, pyrrole–C<sub>3</sub>, C<sub>4</sub>–H), 6.82–6.90 (m, 2H, phenoxy–C<sub>2</sub>, C<sub>6</sub>–H), 7.00–7.08 (m, 2H, phenoxy–C<sub>3</sub>, C<sub>5</sub>–H), 7.47–7.52 (m, 2H, phenyl–C<sub>3</sub>, C<sub>5</sub>–H), 7.79–84 (m, 2H, phenyl–C<sub>2</sub>, C<sub>6</sub>–H), 10.85 (s, 1H, NH); <sup>13</sup>C NMR (100 MHz, DMSO-*d*<sub>6</sub>) δ ppm: 12.35, 13.39, 65.40, 105.95, 115.70, 116.88, 128.09, 129.33, 129.78, 133.19, 140.26, 146.16, 150.68, 150.79, 169.83; MS (ESI): *m/z* = found 377.24 [M<sup>+</sup>]; calcd. 377.17. Anal. Calcd. for C<sub>22</sub>H<sub>23</sub>N<sub>3</sub>O<sub>3</sub>: C, 70.01; H, 6.14; N, 11.13. Found: C, 70.29; H, 6.12; N, 11.17.

**4.7.43. N'-(1-(4-(2,5-Dimethyl-1H-pyrrol-1-yl)phenyl)ethylidene)-2-(4,4,6-trichlorophenoxy)acetohydrazide (**5q**)**

(Yield 60%). mp 244–246 °C; FTIR (KBr): 3182 (NH), 3003, 2925 (Ar–H), 1689 (C=O), 1611 (C=N), 1241 (C–O–C), 750 (C–Cl) cm<sup>-1</sup>; <sup>1</sup>H NMR (400 MHz, DMSO-*d*<sub>6</sub>) δ ppm: 2.00 (s, 6H, 2CH<sub>3</sub>), 2.30 (s, 3H, CH<sub>3</sub>), 5.19 (s, 2H, OCH<sub>2</sub>), 5.81 (s, 2H, pyrrole–C<sub>3</sub>, C<sub>4</sub>–H), 7.44–7.52 (m, 4H, phenoxy–C<sub>3</sub>, C<sub>5</sub>–H and phenyl–C<sub>3</sub>, C<sub>5</sub>–H), 7.87 (m, 2H, phenyl–C<sub>2</sub>, C<sub>6</sub>–H), 10.88 (s, 1H, NH); <sup>13</sup>C NMR (100 MHz, DMSO-*d*<sub>6</sub>) δ ppm: 12.33, 13.38, 65.83, 106.03, 128.03, 129.39, 129.40, 129.85, 129.93, 133.57, 140.89, 145.36, 151.20, 169.93; MS (ESI): *m/z* = found 463.26 [M<sup>+</sup>], 465.10 [M<sup>+</sup> + 2]; calcd. 463.06. Anal. Calcd. for C<sub>22</sub>H<sub>20</sub>Cl<sub>3</sub>N<sub>3</sub>O<sub>2</sub>: C, 56.85; H, 4.34; N, 9.04. Found: C, 56.62; H, 4.36; N, 9.08.

**4.7.44. *N'*-(1-(4-(2,5-Dimethyl-1*H*-pyrrol-1-yl)phenyl)ethylidene)-2-(naphthalen-1-*Y*oxy)acetohydrazide (**5r**)**

(Yield 65%). mp 214–216 °C; FTIR (KBr): 3201 (NH), 3097, 2973, 2920 (Ar—H), 1688 (C=O), 1617 (C=N), 1268 (C—O—C) cm<sup>−1</sup>; <sup>1</sup>H NMR (400 MHz, DMSO-*d*<sub>6</sub>) δ ppm: 2.01 (s, 6H, 2CH<sub>3</sub>), 2.39 (s, 3H, CH<sub>3</sub>), 5.40 (s, 2H, OCH<sub>2</sub>), 5.80 (s, 2H, pyrrole—C<sub>3</sub>, C<sub>4</sub>—H), 6.85 (d, 1H, *J* = 7.5, naphthoxy—C<sub>2</sub>—H), 7.26 (d, 2H, *J* = 8.5, phenyl—C<sub>3</sub>, C<sub>5</sub>—H), 7.35–7.38 (m, 1H, naphthoxy—C<sub>3</sub>—H), 7.43–7.52 (m, 3H, naphthoxy—C<sub>4</sub>, C<sub>6</sub>, C<sub>7</sub>—H), 7.83 (dd, 1H, *J* = 2.2, 3.6, naphthoxy—C<sub>5</sub>—H), 7.94 (d, 2H, *J* = 8.5, phenyl—C<sub>2</sub>, C<sub>6</sub>—H), 8.34 (dd, 1H, *J* = 3.1, 2.5, naphthoxy—C<sub>8</sub>—H), 10.98 (s, 1H, NH); <sup>13</sup>C NMR (100 MHz, DMSO-*d*<sub>6</sub>) δ ppm: 12.81, 13.46, 65.81, 105.99, 107.17, 118.45, 123.51, 125.39, 126.55, 126.82, 127.47, 127.72, 128.63, 129.21, 135.01, 139.23, 147.11, 157.09, 169.37; MS (ESI): *m/z* = found 412.20 [M<sup>+</sup> + 1], 413.21 [M<sup>+</sup> + 2]; calcd. 411.19. Anal. Calcd. for C<sub>26</sub>H<sub>25</sub>N<sub>3</sub>O<sub>2</sub>: C, 75.89; H, 6.12; N, 10.21. Found: C, 75.59; H, 6.14; N, 10.17.

**4.7.45. *N'*-(1-(4-(2,5-Dimethyl-1*H*-pyrrol-1-yl)phenyl)ethylidene)-2-(naphthalen-2-*Y*oxy)acetohydrazide (**5s**)**

(Yield 67%). mp 167–169 °C; FTIR (KBr): 3190 (NH), 3096, 2924 (Ar—H), 1701 (C=O), 1624 (C=N), 1325 (C—O—C) cm<sup>−1</sup>; <sup>1</sup>H NMR (400 MHz, DMSO-*d*<sub>6</sub>) δ ppm: 2.01 (s, 6H, 2CH<sub>3</sub>), 2.39 (s, 3H, CH<sub>3</sub>), 5.32 (s, 2H, OCH<sub>2</sub>), 5.80 (s, 2H, pyrrole—C<sub>3</sub>, C<sub>4</sub>—H), 7.19–7.32 (m, 5H, naphthoxy—C<sub>1</sub>, C<sub>3</sub>, C<sub>6</sub>—H and phenyl—C<sub>3</sub>, C<sub>5</sub>—H), 7.37 (s, 1H, naphthoxy—C<sub>7</sub>—H), 7.73–7.80 (m, 3H, naphthoxy—C<sub>4</sub>, C<sub>5</sub>, C<sub>8</sub>—H), 7.95 (d, 2H, *J* = 8.3, phenyl—C<sub>2</sub>, C<sub>6</sub>—H), 10.97 (s, 1H, NH); <sup>13</sup>C NMR (100 MHz, DMSO-*d*<sub>6</sub>) δ ppm: 12.82, 13.60, 65.59, 106.01, 120.07, 121.81, 124.96, 125.81, 127.21, 127.47, 127.73, 134.01, 137.03, 139.08, 153.78, 169.62; MS (ESI): *m/z* = found 412.20 [M<sup>+</sup> + 1], 413.20 [M<sup>+</sup> + 2]; calcd. 411.19. Anal. Calcd. for C<sub>26</sub>H<sub>25</sub>N<sub>3</sub>O<sub>2</sub>: C, 75.89; H, 6.12; N, 10.21. Found: C, 76.19; H, 6.10; N, 10.17.

**4.7.46. *N'*-(1-(4-(2,5-Dimethyl-1*H*-pyrrol-1-yl)phenyl)ethylidene)-4-methylbenzenesulfonohydrazide (**5t**)**

(Yield 67%). mp 228–230 °C (D); FTIR (KBr): 3206 (NH), 3059, 2926, 2856 (Ar—H), 1597 (C=N), 1336 (SO<sub>2</sub><sup>sym</sup>), 1167 (SO<sub>2</sub><sup>sym</sup>) cm<sup>−1</sup>; <sup>1</sup>H NMR (400 MHz, DMSO-*d*<sub>6</sub>) δ ppm: 1.99 (s, 6H, 2CH<sub>3</sub>), 2.41 (s, 3H, CH<sub>3</sub>), 5.80 (s, 2H, pyrrole—C<sub>3</sub>, C<sub>4</sub>—H), 7.36 (d, 2H, *J* = 8.0, sulfonamidephenyl—C<sub>3</sub>, C<sub>5</sub>—H), 7.42 (d, 2H, *J* = 8.3, phenyl—C<sub>3</sub>, C<sub>5</sub>—H), 7.67 (d, 2H, *J* = 8.2, sulfonamidephenyl—C<sub>2</sub>, C<sub>6</sub>—H), 7.83 (d, 2H, *J* = 8.1, phenyl—C<sub>2</sub>, C<sub>6</sub>—H), 10.32 (s, 1H, NH); <sup>13</sup>C NMR (100 MHz, DMSO-*d*<sub>6</sub>) δ ppm: 12.60, 15.13, 21.05, 106.07, 127.78, 128.01, 129.16, 129.99, 129.53, 135.22, 135.45, 142.22, 143.15, 169.22; MS (ESI): *m/z* = found 381.31 [M<sup>+</sup>]; calcd. 381.15. Anal. Calcd. for C<sub>21</sub>H<sub>23</sub>N<sub>3</sub>O<sub>2</sub>S: C, 66.12; H, 6.08; N, 11.01. Found: C, 66.38; H, 6.06; N, 11.05.

**4.7.47. *N*-(4-((2-(1-(4-(2,5-Dimethyl-1*H*-pyrrol-1-yl)phenyl)ethylidene)hydrazinyl)sulfonyl)phenyl)acetamide (**5u**)**

(Yield 65%). mp 209–211 °C; FTIR (KBr): 3330, 3195 (NH), 3060, 2923 (Ar—H), 1676 (CH<sub>3</sub>C=O), 1595 (C=N), 1323 (SO<sub>2</sub><sup>sym</sup>), 1160 (SO<sub>2</sub><sup>sym</sup>) cm<sup>−1</sup>; <sup>1</sup>H NMR (400 MHz, DMSO-*d*<sub>6</sub>) δ ppm: 1.97 (s, 6H, 2CH<sub>3</sub>), 2.09 (s, 3H, COCH<sub>3</sub>), 2.23 (s, 3H, CH<sub>3</sub>), 5.78 (s, 2H, pyrrole—C<sub>3</sub>, C<sub>4</sub>—H), 7.20 (d, 2H, *J* = 8.5, phenyl—C<sub>3</sub>, C<sub>5</sub>—H), 7.74 (d, 2H, *J* = 8.5, sulfonamidephenyl—C<sub>3</sub>, C<sub>5</sub>—H), 7.79 (d, 2H, *J* = 8.8, sulfonamidephenyl—C<sub>2</sub>, C<sub>6</sub>—H), 7.87 (d, 2H, *J* = 8.8, sulfonamidephenyl—C<sub>2</sub>, C<sub>6</sub>—H), 10.23 (s, 1H, CONH), 10.49 (s, 1H, NH); <sup>13</sup>C NMR (100 MHz, DMSO-*d*<sub>6</sub>) δ ppm: 12.77, 14.09, 105.96, 118.30, 126.60, 127.46, 127.64, 128.51, 132.52, 136.50, 139.08, 143.19, 168.33, 168.77; MS (ESI): *m/z* = found 424.36 [M<sup>+</sup>]; calcd. 424.16. Anal. Calcd. for C<sub>22</sub>H<sub>24</sub>N<sub>4</sub>O<sub>3</sub>S: C, 62.24; H, 5.70; N, 13.20. Found: C, 62.49; H, 5.68; N, 13.15.

**4.7.48. *4-Amino-N'*-(1-(4-(2,5-dimethyl-1*H*-pyrrol-1-yl)phenyl)ethylidene)benzenesulfonohydrazide (**5v**)**

(Yield 60%). mp 230–232 °C; FTIR (KBr): 3358, 3253 (NH), 3108, 2991 (Ar—H), 1514 (C=N), 1347 (SO<sub>2</sub><sup>sym</sup>), 1174 (SO<sub>2</sub><sup>sym</sup>) cm<sup>−1</sup>; <sup>1</sup>H NMR (400 MHz, DMSO-*d*<sub>6</sub>) δ ppm: 1.99 (s, 6H, 2CH<sub>3</sub>), 2.21 (s, 3H, CH<sub>3</sub>), 5.76 (s, 2H, pyrrole—C<sub>3</sub>, C<sub>4</sub>—H), 6.36 (s, 1H, NH<sub>2</sub>), 6.98 (d, 2H, *J* = 8.5, sulfonamidephenyl—C<sub>3</sub>, C<sub>5</sub>—H), 7.45 (d, 2H, *J* = 8.5, phenyl—C<sub>3</sub>, C<sub>5</sub>—H), 7.71 (d, 2H, *J* = 8.8, sulfonamidephenyl—C<sub>2</sub>, C<sub>6</sub>—H), 7.83 (d, 2H, *J* = 8.8, phenyl—C<sub>2</sub>, C<sub>6</sub>—H), 10.38 (s, 1H, NH); <sup>13</sup>C NMR (100 MHz, DMSO-*d*<sub>6</sub>) δ ppm: 12.70, 13.80, 106.03, 112.28, 118.93, 127.07, 128.51, 130.05, 134.01, 136.02, 142.61, 151.60, 168.18; MS (ESI): *m/z* = found 382.55 [M<sup>+</sup>]; calcd. 382.15. Anal. Calcd. for C<sub>20</sub>H<sub>22</sub>N<sub>4</sub>O<sub>2</sub>S: C, 62.80; H, 5.80; N, 14.65. Found: C, 63.05; H, 5.78; N, 14.71.

**4.7.49. 2,5-Dimethyl-1-(4-(1-(2-phenylhydrazono)ethyl)phenyl)-1*H*-pyrrole (**5w**)**

(Yield 65%). mp 180–182 °C; FTIR (KBr): 3214 (NH), 3118, 3044 (Ar—H), 1599 (C=N) cm<sup>−1</sup>; <sup>1</sup>H NMR (400 MHz, DMSO-*d*<sub>6</sub>) δ ppm: 2.00 (s, 6H, 2CH<sub>3</sub>), 2.30 (s, 3H, CH<sub>3</sub>), 5.82 (s, 2H, pyrrole—C<sub>3</sub>, C<sub>4</sub>—H), 6.74–8.08 (m, 9H, hydrazonophenyl—C<sub>2</sub>, C<sub>3</sub>, C<sub>4</sub>, C<sub>5</sub>, C<sub>6</sub>—H and phenyl—C<sub>2</sub>, C<sub>3</sub>, C<sub>5</sub>, C<sub>6</sub>—H), 9.25 (s, 1H, NH); <sup>13</sup>C NMR (100 MHz, DMSO-*d*<sub>6</sub>) δ ppm: 12.60, 13.39, 105.98, 113.73, 113.86, 122.31, 128.03, 129.43, 129.82, 133.84, 140.32, 142.61, 165.02; MS (ESI): *m/z* = found 303.21 [M<sup>+</sup>]; calcd. 303.17. Anal. Calcd. for C<sub>20</sub>H<sub>21</sub>N<sub>3</sub>: C, 79.17; H, 6.98; N, 13.85. Found: C, 78.85; H, 7.01; N, 13.91.

**4.7.50. 1-(4-(1-(2-(2,4-Dinitrophenyl)hydrazono)ethyl)phenyl)-2,5-dimethyl-1*H*-pyrrole (**5x**)**

(Yield 70%). mp 248–250 °C; FTIR (KBr): 3304 (NH), 3101, 2978, 2922 (Ar—H), 1615 (C=N), 1505 (NO<sub>2</sub><sup>sym</sup>), 1267 (NO<sub>2</sub><sup>sym</sup>) cm<sup>−1</sup>; <sup>1</sup>H NMR (400 MHz, DMSO-*d*<sub>6</sub>) δ ppm: 2.03 (s, 6H, 2CH<sub>3</sub>), 2.53 (s, 3H, CH<sub>3</sub>), 5.82 (s, 2H, pyrrole—C<sub>3</sub>, C<sub>4</sub>—H), 7.34 (dd, 2H, *J* = 1.8, 1.6, phenyl—C<sub>3</sub>, C<sub>5</sub>—H), 8.07 (dd, 2H, *J* = 1.8, 1.8, phenyl—C<sub>2</sub>, C<sub>6</sub>—H), 8.18 (t, 1H, *J* = 2.5, dinitrophenyl—C<sub>6</sub>—H), 8.43 (dd, 1H, *J* = 2.5, 2.6, dinitrophenyl—C<sub>5</sub>—H), 8.99 (d, 1H, *J* = 2.6, dinitrophenyl—C<sub>3</sub>—H), 11.24 (s, 1H, NH); <sup>13</sup>C NMR (100 MHz, DMSO-*d*<sub>6</sub>) δ ppm: 12.84, 13.36, 106.17, 116.56, 124.33, 127.25, 127.50, 127.93, 129.97, 130.71, 134.00, 136.15, 142.09, 144.44, 152.01; MS (ESI): *m/z* = found 393.19 [M<sup>+</sup>]; calcd. 393.14. Anal. Calcd. for C<sub>20</sub>H<sub>19</sub>N<sub>5</sub>O<sub>4</sub>: C, 61.06; H, 4.87; N, 17.80. Found: C, 60.82; H, 4.89; N, 17.73.

**4.7.51. 2-(1-(4-(2,5-Dimethyl-1*H*-pyrrol-1-yl)phenyl)ethylidene)hydrazinecarbothioamide (**5y**)**

(Yield 80%). mp 212–214 °C; FTIR (KBr): 3481, 3359, 3173 (NH), 2978, 2912 (Ar—H), 1574 (C=N) cm<sup>−1</sup>; <sup>1</sup>H NMR (400 MHz, DMSO-*d*<sub>6</sub>) δ ppm: 1.99 (s, 6H, 2CH<sub>3</sub>), 2.37 (s, 3H, CH<sub>3</sub>), 5.79 (s, 2H, pyrrole—C<sub>3</sub>, C<sub>4</sub>—H), 7.23 (m, 2H, phenyl—C<sub>3</sub>, C<sub>5</sub>—H), 8.02 (m, 2H, phenyl—C<sub>2</sub>, C<sub>6</sub>—H), 8.26 (s, 2H, NH<sub>2</sub>), 10.23 (s, 1H, NH); <sup>13</sup>C NMR (100 MHz, DMSO-*d*<sub>6</sub>) δ ppm: 12.78, 13.86, 105.93, 127.16, 127.48, 127.52, 136.79, 138.97, 146.58, 178.96; MS (ESI): *m/z* = found 286.61 [M<sup>+</sup>]; calcd. 286.13. Anal. Calcd. for C<sub>15</sub>H<sub>18</sub>N<sub>4</sub>S: C, 62.91; H, 6.33; N, 19.56. Found: C, 63.16; H, 6.30; N, 19.48.

**4.7.52. 2-(1-(4-(2,5-Dimethyl-1*H*-pyrrol-1-yl)phenyl)ethylidene)hydrazinecarboxamide (**5z**)**

(Yield 72%). mp 228–230 °C; FTIR (KBr): 3513, 3398, 3184 (NH), 3122, 2980, 2919 (Ar—H), 1685 (C=O), 1612 (C=N) cm<sup>−1</sup>; <sup>1</sup>H NMR (400 MHz, DMSO-*d*<sub>6</sub>) δ ppm: 2.00 (s, 6H, 2CH<sub>3</sub>), 2.27 (s, 3H, CH<sub>3</sub>), 5.80 (s, 2H, pyrrole—C<sub>3</sub>, C<sub>4</sub>—H), 6.37 (s, 2H, NH<sub>2</sub>), 7.21 (m, 2H, phenyl—C<sub>3</sub>, C<sub>5</sub>—H), 7.90 (m, 2H, phenyl—C<sub>2</sub>, C<sub>6</sub>—H), 9.34 (s, 1H, NH); <sup>13</sup>C NMR (100 MHz, DMSO-*d*<sub>6</sub>) δ ppm: 12.82, 13.22, 105.90, 126.59, 127.45, 127.52, 137.46, 138.26, 143.01, 157.23; MS (ESI): *m/z* = found

270.26 [M<sup>+</sup>]; calcd. 270.15. Anal. Calcd. for C<sub>15</sub>H<sub>18</sub>N<sub>4</sub>O: C, 66.64; H, 6.71; N, 20.73. Found: C, 66.91; H, 6.68; N, 20.81.

## 5. Biological activities

### 5.1. Antitubercular activity

MIC values were determined for *N'*-(1-(4-(2,5-disubstituted-1*H*-pyrrol-1-yl)phenyl)ethylidene)-substituted arylhydrazides (**4a–j** and **5a–j**), *N'*-(1-(4-(2,5-disubstituted-1*H*-pyrrol-1-yl)phenyl)ethylidene)-2-(aryloxy)acetohydrazides (**4k–s** and **5k–s**), *N'*-(1-(4-(2,5-disubstituted-1*H*-pyrrol-1-yl)phenyl)ethylidene)-4-substituted benzene sulfonohydrazides (**4t–v** and **5t–v**), 1-(4-(1-(2-(substitutedphenyl)hydrazone)ethyl)phenyl)-2,5-disubstituted-1*H*-pyrroles (**4w**, **x** and **5w**, **x**) and 2-(1-(4-(2,5-disubstituted-1*H*-pyrrol-1-yl)phenyl)ethylidene)hydrazinecarbothioamide/xamides (**4y**, **z** and **5y**, **z**) against *M. tuberculosis* strain H37Rv using the Microplate Alamar Blue assay (MABA) [42] using isoniazid as the standard drug. The 96 wells plate received 100 µL of Middlebrook 7H9 broth and serial dilution of compounds were made directly on the plate with drug concentrations of 0.2, 0.4, 0.8, 1.6, 3.125, 6.25, 12.5, 25, 50 and 100 µg/mL. Plates were covered and sealed with parafilm and incubated at 37 °C for 5 days. Then, 25 µL of freshly prepared 1:1 mixture of almar blue reagent and 10% Tween 80 was added to the plate and incubated for 24 h. A blue color in the well was interpreted as no bacterial growth and pink color was scored as growth. The MIC was defined as the lowest drug concentration, which prevented color change from blue to pink. Table 1 reveals antitubercular activity (MIC) data.

### 5.2. MTT-based cytotoxic activity

The cellular conversion of MTT [3-(4,5-dimethylthiazolo-2-yl)-2,5-diphenyl-tetrazolium bromide] into a formazan product [43] was used to evaluate cytotoxic activity (IC<sub>50</sub>) of some synthesized compounds against mammalian Vero cell-lines and A<sub>549</sub> (lung adenocarcinoma) cell-lines up to concentrations of 62.5 µg/mL using the Promega Cell Titer 96 non-radioactive cell proliferation assay [44] and cisplatin was the positive control. The IC<sub>50</sub> values are the averages ± SEM of three independent experiments, presented in Table 2.

## 6. Summary

The promising activity of title compounds can be attributed to the incorporation of heterocyclic moieties viz., substituted pyridine,

pyrrole and aromatic compounds with methyl, hydroxy, chloro, bromo, nitro, acetamide and amine groups. The electron rich groups like methyl and hydroxy groups attached to phenyl ring, and methyl substituted pyrrole exhibit a solubilizing effect on the molecule. The halogen substituted aromatic compounds could improve the lipophilic nature of the compounds, while the methoxy substituted compounds would act as electron donor. In addition, the presence of toxophoric –C=NNH– moiety and –C=O group on hydrazone bridge are essential for hydrogen bonding with the receptor, while hydroxyl group at the 4th position of phenyl improves the solubility.

The above mentioned properties of pharmacophores are responsible for the promising activity of the title compounds. When the results of antitubercular activity, docking studies and 3D-QSAR are considered together, it can be suggested that (Fig. 10): (i) the hydrazone moiety, which fills the middle part of pocket in the ENR active site, makes a contribution (NH···OH (Tyr158), C=O···HO (NAD<sup>+</sup>) to hydrogen bonding) to the selectivity. It is a suitable scaffold for InhA enzyme (ii) pyrrole, aryloxy, aroyl, benzenesulphonamide and hydrazone bridge with appropriate substitutions can fill the hydrophobic pocket with residues such as Met155, Ala157, Pro156, Ile215, Leu218, Ala154, Phe149, Met147, Ala198, Phe97, Met161, Met98 and Ile202; which are part of the substrate-binding loop in InhA (Fig. 11), that may be useful to propose new molecules with enhanced selectivity towards InhA enzyme.

## 7. Conclusions

We have accomplished the synthesis of novel derivatives of *N'*-(1-(4-(2,5-disubstituted-1*H*-pyrrol-1-yl)phenyl)ethylidene)-substituted arylhydrazides (**4a–j** and **5a–j**), *N'*-(1-(4-(2,5-disubstituted-1*H*-pyrrol-1-yl)phenyl)ethylidene)-2-(aryloxy)acetohydrazides (**4k–s** and **5k–s**), *N'*-(1-(4-(2,5-disubstituted-1*H*-pyrrol-1-yl)phenyl)ethylidene)-4-substituted benzene sulfonohydrazides (**4t–v** and **5t–v**), 1-(4-(1-(2-(substitutedphenyl)hydrazone)ethyl)phenyl)-2,5-disubstituted-1*H*-pyrroles (**4w**, **x** and **5w**, **x**) and 2-(1-(4-(2,5-disubstituted-1*H*-pyrrol-1-yl)phenyl)ethylidene)hydrazinecarbothioamide/xamides (**4y**, **z** and **5y**, **z**). These pyrrole hydrazones were explored as a new entry in the search for new tuberculostatics, identifying several hydrazones with reasonable inhibitory activities against *M. tuberculosis*. Among all the compounds, **4r–u**, **5k** and **r–u** displayed significant activity (0.2–0.8 µg/mL) against *M. tuberculosis* H37Rv strain. The 3D QSAR studies, CoMFA and CoMSIA models showed high correlative and predictive abilities. A high bootstrapped r<sup>2</sup> value and a small standard deviation indicated that a similar relationship exists in all the compounds. For comparison, two different

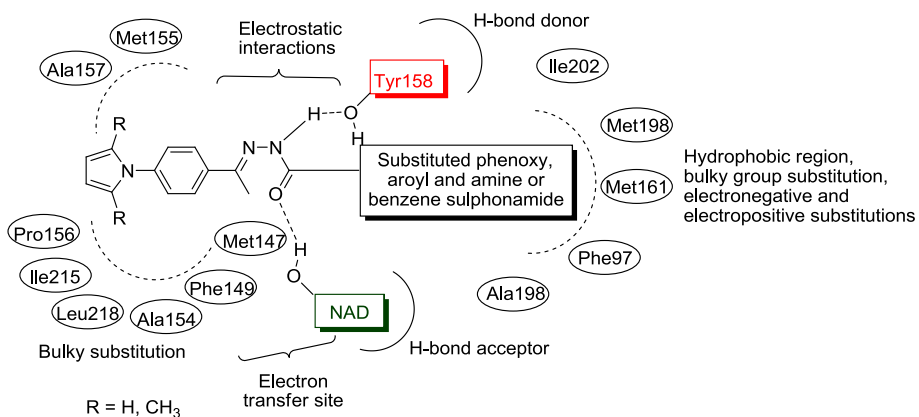


**Fig. 10.** Docked region and structural activity relationship for pyrrole hydrazones. Green residue represents hydrogen bond acceptor, red residues hydrogen bond donors, and black residues form the hydrophobic pocket. (For interpretation of the references to color in this figure legend, the reader is referred to the web version of this article.)

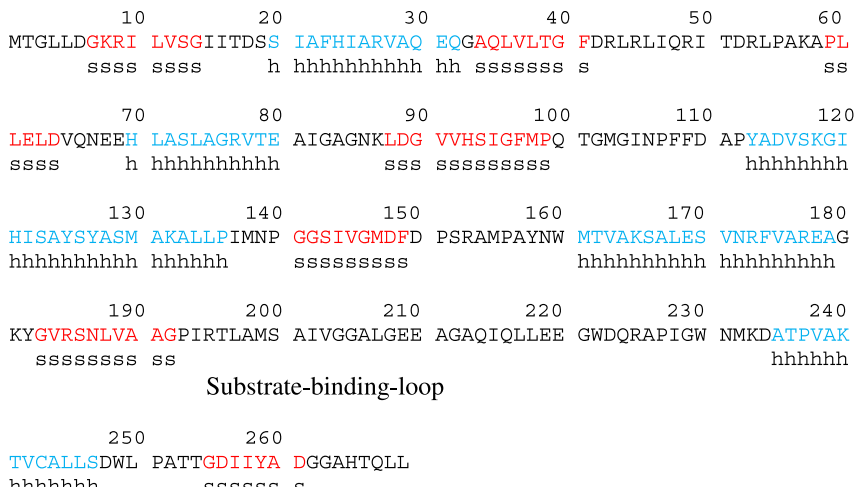


**Fig. 11.** Sequence alignment of FAS-II system enoyl-ACP reductases. The numbering above the alignment corresponds to the *M. tuberculosis* InhA sequence and the lower-case letters below the alignment mark the location of  $\alpha$ -helices (h, light blue) and  $\beta$ -strands (s, red color). The amino acid sequence information was obtained from GenBank™, using accession number *M. tuberculosis*, U02492. (For interpretation of the references to color in this figure legend, the reader is referred to the web version of this article.)

alignment rules including docked alignment and database alignment were used to obtain the 3D-QSAR models that were obtained from the database alignment, which showed better correlation with antitubercular activity and improved predictability.

## Acknowledgments

We thank the research support from Indian Council of Medical Research, New Delhi (File No. 64/4/2011-BMS, IRIS Cell No. 2010-08710). We also thank Mr. H. V. Dambal, President, S. E. T's College of Pharmacy for providing the facilities. We thank Dr. K.G. Bhat of Maratha Mandal's Dental College, Hospital and Research Centre, Belgaum, for providing antitubercular and cytotoxic activities. Director, SAIF, Indian Institute of Technology, Chennai, Tamil Nadu, India and the Director, SAIF, Panjab University, Chandigarh, Panjab, India provided some of the NMR and mass spectral data. The authors are grateful to Mr. S. A. Tiwari for his technical assistance.

## Appendix A. Supplementary data

Supplementary data related to this article can be found at <http://dx.doi.org/10.1016/j.ejmech.2013.11.004>. These data include MOL files and InChiKeys of the most important compounds described in this article.

## References

- [1] A. Pablos-Mendez, M.C. Ravaglione, A. Laszlo, N. Binkin, H.L. Reider, F. Bustreo, D.L. Cohn, C.S. Lambregts-van Weezenbeek, S.J. Kim, P. Chaulet, P. Nunn, N. Engl. J. Med. 338 (1998) 1641–1649.
- [2] WHO Report, Global Tuberculosis Control Surveillance, Financing and Planning, 2010.
- [3] K. Takayama, L. Wang, H.L. David, Antimicrob. Agents Chemother. 2 (1972) 29–35.
- [4] G. Middlebrook, Am. Rev. Tuberc. 65 (1952) 765–767.
- [5] F. Bardou, A. Quemard, M.A. Dupont, C. Horn, G. Marchal, M. Daffe, Antimicrob. Agents Chemother. 40 (1996) 2459–2467.
- [6] Y. Zhang, B. Heym, B. Allen, D. Young, S. Cole, Nature 358 (1992) 591–593.
- [7] A.D. Russell, J. Antimicrob. Chemother. 53 (2004) 693–695.
- [8] H.P. Schweizer, FEMS Microbiol. Lett. 7 (2001) 1–7.
- [9] A.B. Dann, A. Hontela, J. Appl. Toxicol. 31 (2011) 285–311.
- [10] M.J. Stewart, S. Parikh, G. Xiao, P.J. Tonge, C. Kisker, J. Mol. Biol. 290 (1999) 859–865.
- [11] H. Lu, K. England, C. am Ende, J.J. Truglio, S. Luckner, B.G. Reddy, N.L. Marlenee, S.E. Knudson, D.L. Knudson, R.A. Bowen, C. Kisker, R.A. Slayden, P.J. Tonge, ACS Chem. Biol. 4 (2009) 221–231.
- [12] R.D. Cramer, D.E. Patterson, J.D. Bunce, J. Am. Chem. Soc. 110 (1988) 5959.
- [13] H. Kubinyi (Ed.), 3D QSAR in Drug Design: Theory, Methods and Applications, ESCOM Science Publishers, Leiden, 1993.
- [14] G. Klebe, U. Abraham, J. Comput. Aided Mol. Des. 13 (1999) 1–10.
- [15] G. Klebe, U. Abraham, T. Mietzner, J. Med. Chem. 37 (1994) 4130–4146.
- [16] K.K. Bedia, O. Elcin, U. Seda, K. Fatma, S. Nathaly, R. Sevim, A. Dimoglo, Eur. J. Med. Chem. 41 (2006) 1253–1261.
- [17] S. Eswaran, A.V. Adhikari, N.K. Pal, I.H. Chowdhury, Bioorg. Med. Chem. Lett. 20 (2010) 1040–1044.
- [18] J. Vinsova, A. Irmakovskiy, J. Jampilek, J.F. Monreal, M. Dolezal, Anti-Infect. Agents Med. Chem. 7 (2008) 12–31.
- [19] A. Nayyar, A. Malde, E. Coutinho, R. Jain, Bioorg. Med. Chem. 14 (2006) 7302–7310.
- [20] E. Pelttari, E. Karhumaki, J. Langshaw, H. Elo, Z. Naturforschung C J. Biosci. 62 (2007) 483–486.
- [21] H. Yale, K. Losee, J. Martins, M. Holsing, F. Perry, J. Bernstein, J. Am. Chem. Soc. 75 (1953) 1933–1942.
- [22] J. Gazave, N. Buu-Hoi, N. Xuong, J. Mallet, J. Pillot, J. Savel, G. Dufraisse, Therapie 12 (1957) 486–492.
- [23] A. Bijev, Arzneim. Forsch./Drug Res. 59 (1) (2009) 34–39.
- [24] S.D. Joshi, H.M. Vagdevi, V.P. Vaidya, G.S. Gadaginamath, Eur. J. Med. Chem. 43 (2008) 1989–1996.
- [25] M. Biava, G.C. Porretta, G. Poce, A.D. Logu, M. Saddi, R. Meleddu, F. Manetti, E.D. Rossi, M. Botta, J. Med. Chem. 51 (2008) 3644–3648.
- [26] M. Biava, G.C. Porretta, G. Poce, S. Supino, D. Deidda, R. Pompei, P. Molicotti, F. Manetti, M. Botta, J. Med. Chem. 49 (2006) 4946–4952.
- [27] S.D. Joshi, U.A. More, T.M. Aminabhavi, A.M. Badiger, Med. Chem. Res. (21 May 2013), <http://dx.doi.org/10.1007/s00044-013-0607-3>.
- [28] S.D. Joshi, U.A. More, S.R. Dixit, H.H. Korat, T.M. Aminabhavi, A.M. Badiger, Med. Chem. Res. (25 August 2013), <http://dx.doi.org/10.1007/s00044-013-0709-y>.
- [29] D. Deidda, G. Lampis, R. Fioravanti, Antimicrob. Agents Chemother. 2 (1998) 3035–3037.
- [30] S.K. Arora, N. Sinha, R.K. Sinha, R.S. Uppadhyaya, V.M. Modak, A. Tilekar, in: Program and Abstracts of the 44th Interscience Conference on Antimicrobial Agents and Chemotherapy (Washington, DC), American Society for Microbiology, Washington, DC, 2004, p. 212.
- [31] A. Bijev, S. Vladimirova, P. Prodanova, Lett. Drug Des. Discov. 6 (7) (2009) 507–517.
- [32] Tripos International, Sybyl-x 2.0, Tripos International, St. Louis, MO, USA, 2012.
- [33] M. Clark, R.D. Cramer III, N. Van Opdenbosch, J. Comput. Chem. 10 (1989) 982–1012.
- [34] B.L. Bush, R.B. Nachbar, J. Comput. Aided Mol. Des. 7 (1993) 587.
- [35] R.D. Cramer III, J.D. Bunce, D.E. Patterson, I.E. Frank, Quant. Struct. Act Relat. 7 (1988) 18.
- [36] A.N. Jain, J. Comput. Aided Mol. Des. 10 (1996) 427–440.
- [37] A.N. Jain, J. Med. Chem. 46 (2003) 499–511.
- [38] G. Jones, P. Willett, R.C. Glen, A.R. Leach, R. Taylor, J. Mol. Biol. 267 (1997) 727–748.
- [39] I. Muegge, Y.C. Martin, J. Med. Chem. 42 (1999) 791–804.
- [40] I.D. Kuntz, J.M. Blaney, S.J. Oatley, R. Langridge, T.E. Ferrin, J. Mol. Biol. 161 (1982) 269–288.
- [41] M.D. Eldridge, C.W. Murray, T.R. Auton, G.V. Paolini, R.P. Mee, J. Comput. Aided Mol. Des. 11 (1997) 425–445.
- [42] S.G. Franzblau, R.S. Witzig, J.C. McLaughlin, P. Torres, G. Madico, A. Hernandez, M.T. Degnan, M.B. Cook, V.K. Quenzer, R.M. Ferguson, R.H. Gilman, J. Clin. Microbiol. 36 (1998) 362–366.
- [43] T. Mosmann, J. Immunol. Methods 65 (1983) 55–63.
- [44] L.L. Gundersen, J. Nissen-Meyer, B. Spilsberg, J. Med. Chem. 45 (2002) 1383–1386.